Available online at www.sciencedirect.com
ScienceDirect
International Journal of Solids and Structures 44 (2007) 507–529
INTERNATIONAL JOURNAL OF SOLIDS and STRUCTURES
www.elsevier.com/locate/ijsolstr

Effective behavior of linear viscoelastic composites: A time-integration approach

Noël Lahellec *, Pierre Suquet

Laboratoire de Mécanique et d'Acoustique/CNRS, 31 Chemin Joseph Aiguier, 13402 Marseille Cedex 20, France

Received 3 November 2005; received in revised form 21 April 2006
Available online 5 May 2006

Abstract

A new method for determining the overall behavior of composite materials comprised of linear viscoelastic constituents is presented. Unlike classical methods which are based on the Laplace transform, the present method operates directly in the time-domain. Upon use of an implicit time-discretization scheme, the evolution equations describing the constitutive behavior of the phases can be reduced to the minimization of an incremental energy function. This minimization problem is rigorously equivalent to a linear thermoelastic problem with a transformation strain which is a nonuniform field (not even uniform within the phases). The variational technique of Ponte Castañeda is used to approximate the nonuniform eigenstrains by piecewise uniform eigenstrains. The latter problem is amenable to simpler calculations and analytical results for appropriate microstructures can be obtained. The accuracy of the proposed scheme is assessed by comparison of the method with exact results obtained either by full finite element simulations in time-domain or by available analytical results obtained by the Laplace transform.
© 2006 Elsevier Ltd. All rights reserved.

Keywords: Composite; Homogenization; Viscoelasticity; Variational method; Periodic microstructure; Random microstructure; Hashin–Shtrikman bounds

1. Introduction

Many materials, particularly polymers, exhibit a time and rate dependence which can be modelled in the framework of viscoelasticity or viscoplasticity. When these materials are assembled with other constituents to form a composite material, their viscous properties give rise to macroscopic dissipative effects and to damping. Such viscous effects have been studied in polymer-based composites by Papanicolaou et al. (1999) and Houshyar et al. (2005) (poly-propylene-co-ethylene matrix) or Chabert et al. (2004) (polybutylacrylate matrix) among others. They have also been observed in metal–matrix composites at high temperature.

The present study is devoted to the effective behavior of composites made of *linear* viscoelastic phases. There exists an abundant literature on the subject, mostly based on the correspondence principle (Hashin, 1970, for instance). In this approach, the equations governing the local state and the effective properties of

* Corresponding author. Tel.: +33 491 164 208; fax: +33 491 164 481.
E-mail addresses: lahellec@lma.cnrs-mrs.fr (N. Lahellec), suquet@lma.cnrs-mrs.fr (P. Suquet).

0020-7683/$ - see front matter © 2006 Elsevier Ltd. All rights reserved.
doi:10.1016/j.ijsolstr.2006.04.038

linear viscoelastic composites are, after application of the Laplace transform, completely parallel to that of linear elastic composites with complex moduli. Theoretical results and predictive schemes initially developed for elastic composites can be therefore extended to viscoelastic composites by the correspondence principle. This approach has been used for instance by Laws and Mc Laughlin (1978) who applied the self-consistent scheme to viscoelastic constituents. Other micromechanical schemes have been used to estimate the elastic properties of the (fictitious) elastic composites which arise in the Laplace domain, such as the Mori–Tanaka estimate (Brinson and Lin, 1998) or the Hashin–Shtrikman bounds (DeBotton and Tevet-Deree, 2004). General bounds for the complex moduli of viscoelastic composites have been obtained by Gibiansky et al. (1999) using the Hashin–Shtrikman procedure and the translation method.

The use of the Laplace transform has also been crucial in proving that short memory effects in the individual constituents give rise, after homogenization, to long memory effects in the composite (Sanchez-Hubert and Sanchez-Palencia, 1978; Suquet, 1986). A functional theory where the memory effects are accounted for through a creep or relaxation function seems at first to be the most convenient modelling framework to describe such effects. Rougier et al. (1993) have found explicit expressions for the relaxation function of isotropic particulate composites comprised of two different Maxwell materials. However, despite all the findings made possible by the Laplace transform and the correspondence principle, this method has several limitations.

- First, the functional theory of viscoelasticity applied to the effective properties of composites is of limited use for computational purposes. Indeed the implementation of functional constitutive relations requires the storage of all the stress (or strain) history in the composite from the initial time to the present time t. This is a very strong requirement. By contrast, constitutive theories based on internal variables have proved to be more flexible and efficient. In these theories the history of stress and strain (between the initial time and the present time t) is stored in the present value (at time t) of one or several internal variables.
- Second, in many cases of interest the effective complex moduli of the composite in the Laplace domain are not available in closed-form (for instance when the microstructure is complex or when the constituents are anisotropic), and cannot be easily inverted. Therefore the macroscopic creep or relaxation functions can be obtained only through numerical inversion of the Laplace transform (see Yeong-Moo et al. (1998) for a FEM study of periodic media coupled with a numerical inversion of the Laplace transform), an operation which can be costly. For this purpose approximate inversion methods have been proposed (Brenner et al., 2002, for instance), but their use is limited (for good accuracy) to monotone loadings.
- Finally the Laplace transform can be used to convert directly an evolution viscoelastic problem into an equilibrium elastic problem only for linear viscoelasticity. It can also be used indirectly in nonlinear viscoelasticity (Brenner and Masson, 2005) by a suitable linearization of the constitutive relations at each time step (as in Masson and Zaoui (1999)). However, in doing so, the whole history (from $t = 0$ to the present time) of the local stress and strain fields has to be computed at each time step. The present method can be extended directly into a step-by-step method valid for nonlinear problems, where all quantities at the end of the time step are deduced only from those at the beginning of the step. It is the aim of the present study to present a scheme which is both accurate for linear viscoelastic constituents and which can be extended easily to nonlinear viscous effects. This scheme is based on the definition of adequate internal variables at time t. It operates in the time-domain and does not make use of the Laplace transform.

The paper is organized as follows. The constitutive relations used for the individual constituents is presented in Section 2, together with the definition of the exact effective behavior of the composite. An incremental variational principle for a time-discretized version of the evolution equations governing the viscous effects in the composite is derived. It is the building block of the scheme proposed in Section 3. The Euler equations associated with this variational principle are the equations of equilibrium for a linear thermoelastic body subjected to nonuniform eigenstrains (not even uniform within each individual phase). The first step in the proposed approximation is to replace the nonuniform eigenstrains by piecewise uniform (within in each individual phase) eigenstrains. This is done by means of the variational method of Ponte Castañeda (1992), which was initially developed for nonlinear composites but which turns out to be useful in the present linear setting. The resulting thermoelastic problem is therefore a classical problem for a N-phase composite. The accuracy of the proposed scheme is assessed in Section 4 by comparing the predictions of the scheme with exact results both

for random or periodic microstructures. In both cases the results of the proposed scheme are seen to be in excellent agreement with analytical or numerical results.

2. Effective behavior

2.1. Individual constituents

The composite material considered in this study are comprised of individual constituents exhibiting a linear viscoelastic behavior which can be cast in the more general framework of *generalized standard materials*. Their constitutive relations can be derived from two thermodynamic potentials, the free-energy $w(\boldsymbol{\varepsilon},\boldsymbol{\alpha})$ and the dissipation potential $\varphi(\dot{\boldsymbol{\alpha}})$ which are convex functions of the *state variables* and their time-derivative. The state variables are the infinitesimal strain $\boldsymbol{\varepsilon}$ and other internal (scalar or tensorial) internal variables $\boldsymbol{\alpha}$. The formulation of the constitutive relations for generalized standard materials involves two steps.

First, the thermodynamic forces (or driving forces) stored in the material are deduced from the free-energy by derivation with respect to the state variables

$$\boldsymbol{\sigma} = \frac{\partial w}{\partial \boldsymbol{\varepsilon}}(\boldsymbol{\varepsilon},\boldsymbol{\alpha}), \qquad \mathscr{A} = -\frac{\partial w}{\partial \boldsymbol{\alpha}}(\boldsymbol{\varepsilon},\boldsymbol{\alpha}). \tag{1}$$

Second, complementary laws relate the *rate* of the state variables and the forces acting on them. These relations are defined in term of the derivatives of the second potential φ

$$\mathscr{A} = \frac{\partial \varphi}{\partial \dot{\boldsymbol{\alpha}}}(\dot{\boldsymbol{\alpha}}). \tag{2}$$

In summary, the constitutive relations of the materials under consideration in the present study form a system of two differential equations

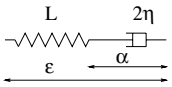
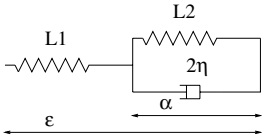
$$\boldsymbol{\sigma} = \frac{\partial w}{\partial \boldsymbol{\varepsilon}}(\boldsymbol{\varepsilon},\boldsymbol{\alpha}), \qquad \frac{\partial w}{\partial \boldsymbol{\alpha}}(\boldsymbol{\varepsilon},\boldsymbol{\alpha}) + \frac{\partial \varphi}{\partial \dot{\boldsymbol{\alpha}}}(\dot{\boldsymbol{\alpha}}) = 0. \tag{3}$$

As schematically recalled in Table 1, most classical viscoelastic models can be formulated in this general framework by appropriate choices of the potentials w and φ.

2.2. Effective response

A representative volume element (r.v.e.) V of the composite is comprised of N phases occupying domains $V^{(r)}$ with characteristic functions $\chi^{(r)}$ and volume fraction $c^{(r)}$. Each individual phase is governed by the

Table 1
Examples of classical linear viscoelastic models and their thermodynamic potentials

Rheological model	Thermodynamic potentials
Maxwell  	$w(\boldsymbol{\varepsilon},\boldsymbol{\alpha}) = \frac{1}{2}(\boldsymbol{\varepsilon}-\boldsymbol{\alpha}) : \boldsymbol{L} : (\boldsymbol{\varepsilon}-\boldsymbol{\alpha})$ $\varphi(\dot{\boldsymbol{\alpha}}) = \eta\dot{\boldsymbol{\alpha}} : \dot{\boldsymbol{\alpha}}.$
Generalized Kelvin–Voigt  	$w(\boldsymbol{\varepsilon},\boldsymbol{\alpha}) = \frac{1}{2}(\boldsymbol{\varepsilon}-\boldsymbol{\alpha}) : \boldsymbol{L}_1 : (\boldsymbol{\varepsilon}-\boldsymbol{\alpha}) + \frac{1}{2}\boldsymbol{\alpha} : \boldsymbol{L}_2 : \boldsymbol{\alpha}$ $\varphi(\dot{\boldsymbol{\alpha}}) = \eta\dot{\boldsymbol{\alpha}} : \dot{\boldsymbol{\alpha}}.$

differential equation (3) with potentials $w^{(r)}$ and $\varphi^{(r)}$. The free-energy w and the dissipation potential φ at position $\boldsymbol{x}$ are given by

$$w(\boldsymbol{x},\boldsymbol{\varepsilon},\boldsymbol{\alpha})=\sum_{r=1}^{N}\chi^{(r)}(\boldsymbol{x})w^{(r)}(\boldsymbol{\varepsilon},\boldsymbol{\alpha}),\qquad \varphi(\boldsymbol{x},\dot{\boldsymbol{\alpha}})=\sum_{r=1}^{N}\chi^{(r)}(\boldsymbol{x})\varphi^{(r)}(\dot{\boldsymbol{\alpha}}).$$

The r.v.e. V is subjected to a path of macroscopic strain $\boldsymbol{E}(t)$ and the local problem which is solved by the local fields $\boldsymbol{\sigma}(\boldsymbol{x},t)$, $\boldsymbol{\varepsilon}(\boldsymbol{x},t)$ and $\boldsymbol{\alpha}(\boldsymbol{x},t)$ reads as

$$\left.\begin{array}{l}\boldsymbol{\sigma}=\dfrac{\partial w}{\partial\boldsymbol{\varepsilon}}(\boldsymbol{\varepsilon},\boldsymbol{\alpha})\quad\text{for }(\boldsymbol{x},t)\in V\times[0,T],\\ \dfrac{\partial w}{\partial\boldsymbol{\alpha}}(\boldsymbol{\varepsilon},\boldsymbol{\alpha})+\dfrac{\partial\varphi}{\partial\dot{\boldsymbol{\alpha}}}(\dot{\boldsymbol{\alpha}})=0\quad\text{for }(\boldsymbol{x},t)\in V\times[0,T],\\ \operatorname{div}\boldsymbol{\sigma}=0\quad\text{for }(\boldsymbol{x},t)\in V\times[0,T],\\ \langle\boldsymbol{\varepsilon}(t)\rangle=\boldsymbol{E}(t)+\text{boundary conditions on }\partial V.\end{array}\right\}\tag{4}$$

All fields $\boldsymbol{\sigma}$, $\boldsymbol{\varepsilon}$, $\boldsymbol{\alpha}$ depend on $\boldsymbol{x}$ and t. The bracket $\langle\cdot\rangle$ denotes spatial averaging over V. For definiteness, periodic boundary conditions are imposed on the boundary of V.

The *homogenized or effective response* of the composite along the path of prescribed strain $\{\boldsymbol{E}(t),\ t\in[0,T]\}$ is the history of average stress $\{\boldsymbol{\Sigma}(t),\ t\in[0,T]\}$.

2.3. Incremental variational principle

Following Lahellec and Suquet (2003), an implicit Euler-scheme can be used to integrate in time Eq. (4).

The interval $[0,T]$ is discretized into time steps $t_0=0,t_1,\ldots,t_n,t_{n+1},\ldots,t_N=T$. Assuming that the fields $\boldsymbol{\sigma}_n$, $\boldsymbol{\varepsilon}_n$ and $\boldsymbol{\alpha}_n$ are known at time t_n, the unknown fields $\boldsymbol{\sigma}_{n+1}$, $\boldsymbol{\varepsilon}_{n+1}$ and $\boldsymbol{\alpha}_{n+1}$ at time t_{n+1} solve a discretized version of the system (4)

$$\left.\begin{array}{l}\boldsymbol{\sigma}_{n+1}=\dfrac{\partial w}{\partial\boldsymbol{\varepsilon}}(\boldsymbol{\varepsilon}_{n+1},\boldsymbol{\alpha}_{n+1})\quad\text{in }V,\\ \dfrac{\partial w}{\partial\boldsymbol{\alpha}}(\boldsymbol{\varepsilon}_{n+1},\boldsymbol{\alpha}_{n+1})+\dfrac{\partial\varphi}{\partial\dot{\boldsymbol{\alpha}}}\left(\dfrac{\boldsymbol{\alpha}_{n+1}-\boldsymbol{\alpha}_n}{\Delta t}\right)=0\quad\text{in }V,\\ \operatorname{div}\boldsymbol{\sigma}_{n+1}=0\quad\text{in }V,\\ \langle\boldsymbol{\varepsilon}_{n+1}\rangle=\boldsymbol{E}_{n+1}+\text{boundary conditions on }\partial V.\end{array}\right\}\tag{5}$$

These equations are the Euler–Lagrange equations for the variational problem

$$\widetilde{J}(\boldsymbol{E}_{n+1})=\inf_{\langle\boldsymbol{\varepsilon}\rangle=\boldsymbol{E}_{n+1}}\ \inf_{\boldsymbol{\alpha}}\langle J(\boldsymbol{\varepsilon},\boldsymbol{\alpha})\rangle,\tag{6}$$

where the incremental potential J is defined as

$$J(\boldsymbol{\varepsilon},\boldsymbol{\alpha})=w(\boldsymbol{\varepsilon},\boldsymbol{\alpha})+\Delta t\,\varphi\left(\frac{\boldsymbol{\alpha}-\boldsymbol{\alpha}_n}{\Delta t}\right).\tag{7}$$

Comments:

1. Note that in (6) the field $\boldsymbol{\varepsilon}$ is constrained by the compatibility conditions, whereas the field $\boldsymbol{\alpha}$ is unconstrained.
2. It should also be noted that, in contrast with w and φ which reduce to $w^{(r)}$ and $\varphi^{(r)}$ in phase r, J is *not* piecewise uniform since it depends on the field $\boldsymbol{\alpha}_n$ which is not necessarily uniform within each individual phase.[1]
3. The average stress $\boldsymbol{\Sigma}_{n+1}=\langle\boldsymbol{\sigma}_{n+1}\rangle$ satisfies

$$\boldsymbol{\Sigma}_{n+1}=\frac{\partial\widetilde{J}}{\partial\boldsymbol{E}}(\boldsymbol{E}_{n+1}).\tag{8}$$

[1] The piecewise uniformity of $w(\boldsymbol{\varepsilon},\boldsymbol{\alpha})$ and $\varphi(\dot{\boldsymbol{\alpha}})$ should be understood in the sense that these potentials are quadratic functions of $(\boldsymbol{\varepsilon},\boldsymbol{\alpha})$ and $\dot{\boldsymbol{\alpha}}$ with piecewise constant coefficients. On the other hand, $J(\boldsymbol{\varepsilon},\boldsymbol{\alpha})$ is a quadratic function of $(\boldsymbol{\varepsilon},\boldsymbol{\alpha})$ with not piecewise uniform coefficients (some of them depending of $\boldsymbol{\alpha}_n$) which is not a piecewise uniform field in general.

Indeed

$$\frac{\partial \widetilde{J}}{\partial \boldsymbol{E}}(\boldsymbol{E}_{n+1}) = \left\langle \frac{\partial J}{\partial \boldsymbol{\varepsilon}} : \frac{\partial \boldsymbol{\varepsilon}}{\partial \boldsymbol{E}} \right\rangle + \left\langle \frac{\partial J}{\partial \boldsymbol{\alpha}} : \frac{\partial \boldsymbol{\alpha}}{\partial \boldsymbol{E}} \right\rangle. \tag{9}$$

The second term vanishes (stationarity with respect to $\boldsymbol{\alpha}$) and the first term reduces to

$$\left\langle \boldsymbol{\sigma}_{n+1} : \frac{\partial \boldsymbol{\varepsilon}}{\partial \boldsymbol{E}} \right\rangle = \langle \boldsymbol{\sigma}_{n+1} \rangle : \left\langle \frac{\partial \boldsymbol{\varepsilon}}{\partial \boldsymbol{E}} \right\rangle = \langle \boldsymbol{\sigma}_{n+1} \rangle.$$

Therefore, after time-discretization, the homogenization of the evolution problem (4) is reduced to the variational problem (6).

3. Approximate homogenization

3.1. Linear viscoelasticity

For simplicity, several working assumptions will be made in the following. They are assumed to hold for each individual constituent of the composite.

H1: The internal state variable $\boldsymbol{\alpha}$ is a symmetric, traceless, second-order tensorial variable.

H2: The free-energy $w^{(r)}$ is a quadratic function of $\boldsymbol{\varepsilon}$ and $\boldsymbol{\alpha}$. It can therefore be written as

$$w^{(r)}(\boldsymbol{\varepsilon}, \boldsymbol{\alpha}) = \frac{1}{2}\boldsymbol{\varepsilon} : \boldsymbol{L}^{(r)}_{\varepsilon\varepsilon} : \boldsymbol{\varepsilon} - \boldsymbol{\alpha} : \boldsymbol{L}^{(r)}_{\varepsilon\alpha} : \boldsymbol{\varepsilon} + \frac{1}{2}\boldsymbol{\alpha} : \boldsymbol{L}^{(r)}_{\alpha\alpha} : \boldsymbol{\alpha}, \tag{10}$$

where the fourth-order tensors $\boldsymbol{L}^{(r)}_{\varepsilon\varepsilon}$, $\boldsymbol{L}^{(r)}_{\varepsilon\alpha}$ and $\boldsymbol{L}^{(r)}_{\alpha\alpha}$ have minor and major symmetries characterized by

$$L_{ijkh} = L_{jikh} = L_{khij}.$$

H3: The constituents are isotropic. As a consequence the fourth-order tensors $\boldsymbol{L}^{(r)}_{\varepsilon\varepsilon}$, $\boldsymbol{L}^{(r)}_{\varepsilon\alpha}$ and $\boldsymbol{L}^{(r)}_{\alpha\alpha}$ can be characterized by two elastic moduli (a bulk modulus and a shear modulus)

$$\boldsymbol{L}_{\theta\gamma} = 3k_{\theta\gamma}\boldsymbol{J} + 2\mu_{\theta\gamma}\boldsymbol{K},$$

where $\boldsymbol{J}$ and $\boldsymbol{K}$ are two orthogonal projectors, corresponding to the projection on spherical tensors and deviators respectively. Similarly, the dissipation potential can be characterized by a single scalar coefficient (recall that the internal variable $\boldsymbol{\alpha}$ is traceless)

$$\varphi^{(r)}(\dot{\boldsymbol{\alpha}}) = \eta^{(r)}\dot{\boldsymbol{\alpha}} : \dot{\boldsymbol{\alpha}}. \tag{11}$$

Comments:

1. H1 is in particular satisfied when the only internal variable is the anelastic strain.
2. Assumption H2 is met by the two models presented in Table 1.

3.2. Variational method

To simplify the notations, the dependence in time of the unknown fields at time t_{n+1} will be omitted from now on. In other words $\boldsymbol{\sigma}_{n+1}$, $\boldsymbol{\varepsilon}_{n+1}$, $\boldsymbol{\alpha}_{n+1}$ will be simply denoted as $\boldsymbol{\sigma}$, $\boldsymbol{\varepsilon}$ and $\boldsymbol{\alpha}$.

The idea of the variational method due to Ponte Castañeda (1992) is to add and subtract to the original energy J which is difficult to homogenize, an energy J_0 which is more amenable to homogenization, while the difference $J - J_0$ can still be estimated. The reference energy J_0 is chosen to be piecewise uniform,

$$J_0(\boldsymbol{x}, \boldsymbol{\varepsilon}, \boldsymbol{\alpha}) = \sum_{r=1}^{N} J_0^{(r)}(\boldsymbol{\varepsilon}, \boldsymbol{\alpha})\chi^{(r)}(\boldsymbol{x}),$$

where

$$J_0^{(r)}(\boldsymbol{\varepsilon}, \boldsymbol{\alpha}) = w^{(r)}(\boldsymbol{\varepsilon}, \boldsymbol{\alpha}) + \frac{\eta_0^{(r)}}{\Delta t}(\boldsymbol{\alpha} - \boldsymbol{\alpha}_n^{(r)}) : (\boldsymbol{\alpha} - \boldsymbol{\alpha}_n^{(r)}). \tag{12}$$

In this expression $\eta_0^{(r)}$ and $\boldsymbol{\alpha}_n^{(r)}$ are uniform in phase r and will be chosen appropriately in the sequel. It is convenient in the forthcoming analysis to introduce a non-dimensional unknown $\theta^{(r)}$ defined as

$$\eta_0^{(r)} = \theta^{(r)}\eta^{(r)}.$$

Let ΔJ be the difference between J and J_0. Then (6) can be re-written as

$$\widetilde{J}(\boldsymbol{E}) = \inf_{\langle\boldsymbol{\varepsilon}\rangle=\boldsymbol{E}} \left[\inf_{\boldsymbol{\alpha}} \langle J_0(\boldsymbol{\varepsilon},\boldsymbol{\alpha}) + \Delta J(\boldsymbol{\alpha})\rangle\right] \leqslant \inf_{\langle\boldsymbol{\varepsilon}\rangle=\boldsymbol{E}} \left[\inf_{\boldsymbol{\alpha}} \langle J_0(\boldsymbol{\varepsilon},\boldsymbol{\alpha})\rangle + \langle \sup_{\boldsymbol{\alpha}} \Delta J(\boldsymbol{\alpha})\rangle\right]. \tag{13}$$

The last expression, where the supremum of ΔJ over $\boldsymbol{\alpha}$ is taken, provides a rigorous upper bound for $\widetilde{J}$. It has been recognized in other situations (Ponte Castañeda and Willis, 1999; Ponte Castañeda, 2002) that a sharper estimate can be obtained by requiring only *stationarity* of ΔJ with respect to $\boldsymbol{\alpha}$ in (13). The resulting expression has no upper bound character and is only an estimate (hopefully accurate) of $\widetilde{J}$

$$\widetilde{J}(\boldsymbol{E}) \approx \inf_{\langle\boldsymbol{\varepsilon}\rangle=\boldsymbol{E}} \left[\inf_{\boldsymbol{\alpha}} \langle J_0(\boldsymbol{\varepsilon},\boldsymbol{\alpha})\rangle + \left\langle \operatorname*{Stat}_{\boldsymbol{\alpha}} \Delta J(\boldsymbol{\alpha})\right\rangle\right]. \tag{14}$$

The stationarity problem to be solved reads, at each point $\boldsymbol{x}$

$$\operatorname*{Stat}_{\boldsymbol{\alpha}} \frac{\eta^{(r)}}{\Delta t}(\boldsymbol{\alpha}-\boldsymbol{\alpha}_n) : (\boldsymbol{\alpha}-\boldsymbol{\alpha}_n) - \frac{\eta^{(r)}\theta^{(r)}}{\Delta t}(\boldsymbol{\alpha}-\boldsymbol{\alpha}_n^{(r)}) : (\boldsymbol{\alpha}-\boldsymbol{\alpha}_n^{(r)}),$$

which gives

$$\boldsymbol{\alpha}(\boldsymbol{x}) = \frac{\boldsymbol{\alpha}_n(\boldsymbol{x}) - \theta^{(r)}\boldsymbol{\alpha}_n^{(r)}}{1-\theta^{(r)}}.$$

With this relation, the estimate (14) becomes

$$\widetilde{J}(\boldsymbol{E}) \approx \inf_{\langle\boldsymbol{\varepsilon}\rangle=\boldsymbol{E}} \left[\inf_{\boldsymbol{\alpha}} \langle J_0(\boldsymbol{\varepsilon},\boldsymbol{\alpha})\rangle\right] + \left\langle \frac{\eta^{(r)}\theta^{(r)}}{\Delta t(\theta^{(r)}-1)}(\boldsymbol{\alpha}_n-\boldsymbol{\alpha}_n^{(r)}) : (\boldsymbol{\alpha}_n-\boldsymbol{\alpha}_n^{(r)})\right\rangle. \tag{15}$$

This estimate can again be optimized with respect to $\theta^{(r)}$ and $\boldsymbol{\alpha}_n^{(r)}$ which have not yet been specified. Stationarity of the right-hand side of (15) with respect to these variables yields

$$\frac{\partial}{\partial\theta^{(r)}}\left\langle J_0^{(r)}(\boldsymbol{\varepsilon},\boldsymbol{\alpha}) + \frac{\eta^{(r)}\theta^{(r)}}{\Delta t(\theta^{(r)}-1)}(\boldsymbol{\alpha}_n-\boldsymbol{\alpha}_n^{(r)}) : (\boldsymbol{\alpha}_n-\boldsymbol{\alpha}_n^{(r)})\right\rangle = 0$$

$$\Rightarrow \quad \theta^{(r)} = 1 \pm \sqrt{\frac{\left\langle (\boldsymbol{\alpha}_n-\boldsymbol{\alpha}_n^{(r)}) : (\boldsymbol{\alpha}_n-\boldsymbol{\alpha}_n^{(r)})\right\rangle_r}{\left\langle (\boldsymbol{\alpha}-\boldsymbol{\alpha}_n^{(r)}) : (\boldsymbol{\alpha}-\boldsymbol{\alpha}_n^{(r)})\right\rangle_r}} \tag{16}$$

and

$$\frac{\partial}{\partial\boldsymbol{\alpha}_n^{(r)}}\left\langle J_0^{(r)}(\boldsymbol{\varepsilon},\boldsymbol{\alpha}) + \frac{\eta^{(r)}\theta^{(r)}}{\Delta t(\theta^{(r)}-1)}(\boldsymbol{\alpha}_n-\boldsymbol{\alpha}_n^{(r)}) : (\boldsymbol{\alpha}_n-\boldsymbol{\alpha}_n^{(r)})\right\rangle = 0$$

$$\Rightarrow \quad \boldsymbol{\alpha}_n^{(r)} = \frac{\langle\boldsymbol{\alpha}_n\rangle_r + (\theta^{(r)}-1)\langle\boldsymbol{\alpha}\rangle_r}{\theta^{(r)}}, \tag{17}$$

where $\langle\cdot\rangle_r$ denotes the spatial average over phase r.

Comments:

1. The internal variable $\boldsymbol{\alpha}_n^{(r)}$, which can be interpreted at first as the effective internal variable at time t_n, is a function of $\boldsymbol{\alpha}$ which is defined only at time t_{n+1}. This definition does not violate the causality principle since $\boldsymbol{\alpha}_n^{(r)}$ is used only at time t_{n+1}. Therefore one should not consider $\boldsymbol{\alpha}_n^{(r)}$ as the effective internal variable at time t_n, but as the internal variable summarizing the history of the internal variable $\boldsymbol{\alpha}$ up to t_{n+1}. Its proper interpretation is that $(\boldsymbol{\alpha}-\boldsymbol{\alpha}_n^{(r)})/\Delta t$ is an approximation of $\dot{\boldsymbol{\alpha}}$ at time t_{n+1}.

2. The equation expressing the optimality condition for $\theta^{(r)}$ has two roots. The root defined by (16) with a + corresponds to the maximum of ΔJ and the one defined with a − correspond to the minimum of ΔJ. These roots give respectively a rigorous upper bound and a rigorous lower bounds for $\widetilde{J}$. The latter result can be seen by noting that

$$\widetilde{J}(\boldsymbol{E}) \geqslant \inf_{\langle\boldsymbol{\varepsilon}\rangle=\boldsymbol{E}} \left[\inf_{\boldsymbol{\alpha}} \langle J_0(\boldsymbol{\varepsilon},\boldsymbol{\alpha})\rangle\right] + \left\langle \inf_{\boldsymbol{\alpha}} \Delta J(\boldsymbol{\alpha})\right\rangle.$$

The estimates obtained for the effective stress given by the two roots are compared with exact results for two-dimensional periodic composites in Section 4.3. Fig. 3 shows that the lower bound, denoted Model$^-$ (FEM), is very close to the exact results (up to numerical error) denoted Exact (FEM), whereas the upper bound, denoted Model$^+$ (FEM), deviates significantly from the exact solution. The lower bound will be retained in the subsequent discussion.

The expression (15) can be further simplified by eliminating $\boldsymbol{\alpha}$. The field $\boldsymbol{\alpha}$ solution of the infimum problem in (15) is given by

$$\boldsymbol{\alpha}(\boldsymbol{x}) = \frac{\mu_{\varepsilon\alpha}^{(r)}}{\mu_{\alpha\alpha}^{(r)} + \eta^{(r)}\theta^{(r)}/\Delta t}\boldsymbol{K} : \boldsymbol{\varepsilon}(\boldsymbol{x}) + \frac{\eta^{(r)}\theta^{(r)}/\Delta t}{\mu_{\alpha\alpha}^{(r)} + \eta^{(r)}\theta^{(r)}/\Delta t}\boldsymbol{\alpha}_n^{(r)}. \tag{18}$$

Upon substitution of this expression in (15), one obtains

$$\widetilde{J}(\boldsymbol{E}) \approx \widetilde{W}_\Delta(\boldsymbol{E}) + \left\langle \frac{\eta^{(r)}\theta^{(r)}}{\Delta t(\theta^{(r)}-1)}(\boldsymbol{\alpha}_n - \boldsymbol{\alpha}_n^{(r)}) : (\boldsymbol{\alpha}_n - \boldsymbol{\alpha}_n^{(r)})\right\rangle. \tag{19}$$

In this expression $\widetilde{W}_\Delta$ is the effective energy of an auxiliary thermoelastic problem which reads

$$\widetilde{W}_\Delta(\boldsymbol{E}) = \inf_{\langle\boldsymbol{\varepsilon}\rangle=\boldsymbol{E}} \langle w_\Delta^{(r)}(\boldsymbol{\varepsilon})\rangle, \qquad w_\Delta^{(r)}(\boldsymbol{\varepsilon}) = \frac{1}{2}\boldsymbol{\varepsilon} : \mathscr{L}^{(r)} : \boldsymbol{\varepsilon} + \boldsymbol{\tau}^{(r)} : \boldsymbol{\varepsilon} + f^{(r)}, \tag{20}$$

where the tensors $\mathscr{L}^{(r)}$ and $\boldsymbol{\tau}^{(r)}$ and the energy $f^{(r)}$ are piecewise uniform and defined as

$$\left.\begin{aligned} \mathscr{L}^{(r)} &= 3k_{\varepsilon\varepsilon}^{(r)}\boldsymbol{J} + 2\left(\mu_{\varepsilon\varepsilon}^{(r)} - \frac{(\mu_{\varepsilon\alpha}^{(r)})^2}{\mu_{\alpha\alpha}^{(r)} + \eta^{(r)}\theta^{(r)}/\Delta t}\right)\boldsymbol{K} \overset{\text{def}}{=} 3k_\Delta^{(r)}\boldsymbol{J} + 2\mu_\Delta^{(r)}\boldsymbol{K}, \\ \boldsymbol{\tau}^{(r)} &= -\frac{2\mu_{\varepsilon\alpha}^{(r)}\eta^{(r)}\theta^{(r)}}{\Delta t\mu_{\alpha\alpha}^{(r)} + \eta^{(r)}\theta^{(r)}}\boldsymbol{\alpha}_n^{(r)}, \qquad f^{(r)} = \frac{\mu_{\alpha\alpha}^{(r)}\eta^{(r)}\theta^{(r)}}{\Delta t\mu_{\alpha\alpha}^{(r)} + \eta^{(r)}\theta^{(r)}}\boldsymbol{\alpha}_n^{(r)} : \boldsymbol{\alpha}_n^{(r)}. \end{aligned}\right\} \tag{21}$$

3.3. Thermoelasticity problem

Relations (16) and (17) involve the first and second moments of $\boldsymbol{\alpha}$ which can be obtained through (18) from the first and second moments of $\boldsymbol{\varepsilon}$ (and more specifically of its deviator, since $\boldsymbol{\alpha}$ is deviatoric) solution of (20).

The first moment of $\boldsymbol{\varepsilon}$ can be expressed by means of the classical localization tensors $\boldsymbol{A}^{(r)}$ and $\boldsymbol{a}^{(r)}$ (see, for instance, Willis, 1981) as follows:

$$\langle\boldsymbol{\varepsilon}\rangle_r = \boldsymbol{A}^{(r)} : \boldsymbol{E} + \boldsymbol{a}^{(r)}. \tag{22}$$

The second moment can be obtained from the effective energy by the relations (Kreher and Pompe, 1985; Suquet, 1995)

$$\langle\boldsymbol{\varepsilon}^{\mathrm{d}} : \boldsymbol{\varepsilon}^{\mathrm{d}}\rangle_r = \frac{1}{c_r}\frac{\partial\widetilde{W}_\Delta}{\partial\mu_\Delta^{(r)}}, \tag{23}$$

where $\boldsymbol{\varepsilon}^{\mathrm{d}}$ denotes the deviator of $\boldsymbol{\varepsilon}$. The expression of the effective energy for thermoelastic composites can be found in Willis (1981)

$$\widetilde{W}_\Delta(\boldsymbol{E}) = \frac{1}{2}\boldsymbol{E} : \widetilde{\mathscr{L}} : \boldsymbol{E} + \widetilde{\boldsymbol{\tau}} : \boldsymbol{E} + \tilde{f}, \tag{24}$$

where

$$\widetilde{\mathscr{L}} = \langle \mathscr{L} \rangle + \sum_{r=1}^{n-1} c_r (\mathscr{L}^{(r)} - \mathscr{L}^{(n)}) : (\boldsymbol{A}^{(r)} - \boldsymbol{I}), \tag{25}$$

$$\widetilde{\boldsymbol{\tau}} = \langle \boldsymbol{\tau} \rangle + \sum_{r=1}^{n-1} c_r (\boldsymbol{A}^{(r)} - \boldsymbol{I})^T : (\boldsymbol{\tau}^{(r)} - \boldsymbol{\tau}^{(n)}), \tag{26}$$

$$\tilde{f} = \langle f \rangle + \sum_{r=1}^{n-1} c_r (\boldsymbol{\tau}^{(r)} - \boldsymbol{\tau}^{(n)}) : \boldsymbol{a}^{(r)}. \tag{27}$$

These expressions simplify significantly for two-phase composites. According to Levin's (1967) relations, the localization operators can be explicitly expressed in terms of the effective properties

$$\boldsymbol{A}^{(1)} = \boldsymbol{I} + \frac{1}{c_1} (\mathscr{L}^{(1)} - \mathscr{L}^{(2)})^{-T} : (\widetilde{\mathscr{L}} - \langle \mathscr{L} \rangle)^{\mathrm{T}}, \tag{28}$$

$$\boldsymbol{a}^{(1)} = \frac{1}{c_1} (\mathscr{L}^{(1)} - \mathscr{L}^{(2)})^{-1} : (\widetilde{\mathscr{L}} - \langle \mathscr{L} \rangle) : (\mathscr{L}^{(1)} - \mathscr{L}^{(2)})^{-1} : (\boldsymbol{\tau}^{(1)} - \boldsymbol{\tau}^{(2)}). \tag{29}$$

It follows from these relations that the effective thermoelastic energy of the composite can be expressed in terms of the effective stiffness of the composite only

$$\widetilde{W}_{\Delta} = \langle f \rangle + \langle \boldsymbol{\tau} \rangle : \boldsymbol{E} + \frac{1}{2} \boldsymbol{E} : \langle \mathscr{L} \rangle : \boldsymbol{E} + \frac{1}{2} [\boldsymbol{E} + (\Delta \mathscr{L})^{-1} : \Delta \boldsymbol{\tau}] : (\widetilde{\mathscr{L}} - \langle \mathscr{L} \rangle) : [\boldsymbol{E} + (\Delta \mathscr{L})^{-1} : \Delta \boldsymbol{\tau}], \tag{30}$$

where

$$\Delta \mathscr{L} = \mathscr{L}^{(1)} - \mathscr{L}^{(2)}, \qquad \Delta \boldsymbol{\tau} = \boldsymbol{\tau}^{(1)} - \boldsymbol{\tau}^{(2)}.$$

The effective stiffness can either be computed numerically, or estimated by an analytical scheme appropriate for the composite microstructure under consideration.

3.4. Effective response of the composite

The procedure for determining the effective response of the composite goes as follows:

1. At time t_n, the first moment $\langle \boldsymbol{\alpha}_n \rangle_r$ and the second moment $\langle \boldsymbol{\alpha}_n : \boldsymbol{\alpha}_n \rangle_r$ of the internal variables are known for each individual phase r.
2. The effective incremental energy $\widetilde{J}$ is estimated through relation (19) and (20).
3. These expressions involve known quantities such as the second moment of $\boldsymbol{\alpha}_n$ available from the previous time step, and unknown quantities such as $\theta^{(r)}$ and $\boldsymbol{\alpha}_n^{(r)}$.
4. These unknown quantities are related through (16) and (17) to the first and second moment per phase of the unknown field of internal variable $\boldsymbol{\alpha}$ at time t_{n+1}. These moments are themselves related through (18) to the first and second moment of the strain field $\boldsymbol{\varepsilon}$ solution of the thermoelasticity problem (20).
5. This first and second moment of the strain are deduced from relations (22)–(24). These moments depend on the thermoelastic constants (21) which also depend on the unknown quantities $\theta^{(r)}$ and $\boldsymbol{\alpha}_n^{(r)}$.
6. Therefore an implicit system of (nonlinear) equations is to be solved for $\theta^{(r)}$ and $\boldsymbol{\alpha}_n^{(r)}$. The first and second moment of $\boldsymbol{\alpha}$ in each individual phase can be deduced from the solution of this set of equations.
7. Finally, the macroscopic stress $\boldsymbol{\Sigma}_{n+1}$ is obtained by taking the average of the microscopic stress field

$$\boldsymbol{\Sigma}_{n+1} = \langle \boldsymbol{\sigma}_{n+1} \rangle = \sum_{r=1}^{n} c_r \left[\mathscr{L}^{(r)} : \langle \boldsymbol{\varepsilon} \rangle_r + \boldsymbol{\tau}^{(r)} \right] = \sum_{r=1}^{n} c_r \left[\mathscr{L}^{(r)} : (\boldsymbol{A}^{(r)} : \boldsymbol{E}_{n+1} + \boldsymbol{a}^{(r)}) + \boldsymbol{\tau}^{(r)} \right] \tag{31}$$

where $\boldsymbol{\tau}^{(r)}$, $\boldsymbol{a}^{(r)}$ and $\boldsymbol{A}^{(r)}$ are defined in (21) and (22), respectively.

4. Application to the in-plane response of fiber composites

In this section, the accuracy of the present model is assessed by comparison of the predictions of the present model with the *exact* response of specific classes of microstructures. These exact results can be obtained either analytically for specific microstructures or numerically for general periodic microstructures.

In what follows the focus will be on two-phase fiber composites. The fibers, aligned with the x_3 axis, will be identified as phase 1, whereas the continous phase, called the matrix, will be identified as phase 2. The problem is two-dimensional and the loading is an imposed macroscopic shear strain

$$\boldsymbol{E}(t) = E_{11}(t)\boldsymbol{e}_1 \otimes \boldsymbol{e}_1 - E_{11}(t)\boldsymbol{e}_2 \otimes \boldsymbol{e}_2. \tag{32}$$

The strain history $E_{11}(t)$ depends on the type of loading under consideration (monotone loading or cyclic loading) and will be specified in due time.

4.1. Different levels of approximation

As in nonlinear homogenization,[2] there are two levels of approximation involved in the practical implementation of the model (besides the time-integration method which will not be discussed here).

1. A first approximation is made in relation (15) where the exact effective incremental potential is replaced by an approximate potential involving a secant viscosity $\eta^{(r)}\theta^{(r)}$ and an effective internal variable $\boldsymbol{\alpha}_n^{(r)}$ for each phase. This approximation is central in the present study and is the one that we would like to evaluate.
2. The second source of approximation lies in the evaluation of the effective energy of the thermoelastic composite (20).

To evaluate separately the two types of error, two types of microstructures were considered

- Microstructures for which the effective energy (20) of the thermoelastic composite can be obtained in closed-form. Assume for instance that the microstructure under consideration is such that its effective properties are *exactly* predicted by a specific micromechanical (one of the Hashin and Shtrikman bounds in our case). Then the effective tensors $\widetilde{\mathscr{L}}$, $\widetilde{\boldsymbol{\tau}}$ and the scalar $\widetilde{f}$ entering relation (20) are known in closed-form. Similarly the exact viscoelastic response of the composite is known by means of the Laplace transform. Therefore comparisons can be made with the model in which the only approximation involved is due to the introduction of the effective variable $\boldsymbol{\alpha}_n^{(r)}$. Section 4.2 is devoted to this special class of microstructures.
- Periodic microstructures which are too complex to allow for an exact determination of their effective properties in closed-form. These effective properties have to be either computed numerically (by the finite element method in our case) or approximated by a micromechanical scheme relevant to the microstructure under consideration. For periodic two-phase composites, where one phase is dispersed in the other, the Hashin–Shtrikman *estimate* (it is not an exact prediction for general periodic microstructures) is a natural candidate for this purpose. The first method (numerical resolution of the thermoelastic problem) does not introduce any additional error but requires the use of a FEM code. The second method has the advantage of being analytical (for random microstructures) or semi-analytical (for periodic microstructures). It is therefore easy to implement and inexpensive. However it introduces another error in addition to the one that we would like to evaluate.

4.2. Microstructures realizing the Hashin–Shtrikman bound

The microstructures considered in this section are such that their effective linear elastic properties are *exactly* given by one of the Hashin–Shtrikman bounds. Consider first the case where the individual phases

[2] The problem considered here is a linear viscoelasticity problem, but as explained in Section 3.2 it shares many features with nonlinear homogenization.

are isotropic, incompressible and characterized by a shear modulus $\mu^{(r)}$ in phase r. The composite is assumed to have overall transverse isotropy and its effective elastic properties are characterized by a single shear modulus $\tilde{\mu}$. The Hashin–Shtrikman bound retained in the subsequent analysis reads as

$$\tilde{\mu}^{\mathrm{HS}} = \frac{\mu^{(2)}\mu^{(1)} + \mu^{(2)}\left(c_1\mu^{(1)} + c_2\mu^{(2)}\right)}{\mu^{(2)} + c_2\mu^{(1)} + c_1\mu^{(2)}}, \tag{33}$$

where $\mu^{(1)}$ and $\mu^{(2)}$ denote respectively the shear moduli of the inclusion and of the matrix. Francfort and Murat (1986) have provided an explicit construction of microstructures whose effective properties are *exactly* $\tilde{\mu}^{\mathrm{HS}}$. We shall consider such a microstructure in the sequel.

We turn now to composites where the individual phases are linear viscoelastic of Maxwell type (see Table 1). They are assumed to be isotropic and incompressible. System (4) can be solved in the Laplace domain (DeBotton and Tevet-Deree, 2004; Barbero and Luciano, 1995). Recalling that the Laplace transform of a time dependent function f is given by

$$L[f(t)] = \hat{f}(p) = \int_0^\infty f(t)\mathrm{e}^{-pt}\,\mathrm{d}t \quad \text{with } p \text{ a complex variable}, \tag{34}$$

the equations for a Maxwell material read in the Laplace domain

$$\hat{\boldsymbol{\sigma}}^{\mathrm{d}} = 2\hat{\mu}(p) : \hat{\boldsymbol{\varepsilon}}^{\mathrm{d}} \quad \text{with } \hat{\mu}(p) = \frac{p\mu}{\frac{\mu}{\eta} + p}, \tag{35}$$

where the superscript d denotes the deviatoric part of a tensor.

The material data chosen for the two phases are

$$\begin{aligned} &\text{viscoelastic Maxwell matrix:} \quad 2\mu^{(2)} = 46.6\ \mathrm{GPa}, \quad \eta^{(2)} = 10\ \mathrm{GPa\,s}, \\ &\text{Elastic fibers:} \quad 2\mu^{(1)} = 266.6\ \mathrm{GPa}. \end{aligned} \tag{36}$$

The loading is an in-plane shear strain as specified in (32). Three regimes can be observed in the response of viscoelastic composites under general monotone conditions: the instantaneous response (when t is close to 0), the response at large time (when t tends to $+\infty$) and, in between, the transient response. The responses at small and large time are characterized by linear operators $\widetilde{\boldsymbol{L}}^A$ and $\widetilde{\boldsymbol{L}}^B$ (Vinogradov and Milton, 2005) which do not depend on the loading conditions and are the effective tensors associated with the corresponding tensors $\mathbf{L}^{(r),A}$ and $\boldsymbol{L}^{(r),B}$ for the individual phases. By contrast, the transient response of the composite depends on loading conditions.

4.2.1. Effective harmonic shear modulus

In this section the composite is subjected to sinusoidal cycles (see Fig. 1(a)), defined by

$$E_{11}(t) = \begin{cases} 5\times 10^{-3}\omega t & \text{for } t < \dfrac{15}{\omega}s, \\ 7.5\times 10^{-2} + 5\times 10^{-3}\sin(\omega t - 15) & \text{for } t \geqslant \dfrac{15}{\omega}s, \end{cases} \tag{37}$$

ω is the frequency of the loading.

The response of the composite subjected to a cyclic loading in the form $\boldsymbol{E}(t) = \bar{\boldsymbol{e}} + \boldsymbol{e}\sin(\omega t)$, see Fig. 1(a), is given by $\widetilde{\boldsymbol{L}}^B$ when $\omega \to 0$, by $\widetilde{\boldsymbol{L}}^A$ when $\omega \to \infty$ and by an effective harmonic modulus $\widetilde{\boldsymbol{L}}(\omega)$ intermediate between the two limit values $\widetilde{\boldsymbol{L}}^A$ and $\widetilde{\boldsymbol{L}}^B$. The asymptotic response of the composite (as t tends to $+\infty$) is in the form $\boldsymbol{\Sigma}(t) = \bar{\boldsymbol{s}} + \boldsymbol{s}\sin(\omega t + \phi)$, where ϕ is the phase shift between the macroscopic strain and stress. The effective harmonic modulus is given by

$$\boldsymbol{s} = \widetilde{\boldsymbol{L}}(\omega) : \boldsymbol{e}. \tag{38}$$

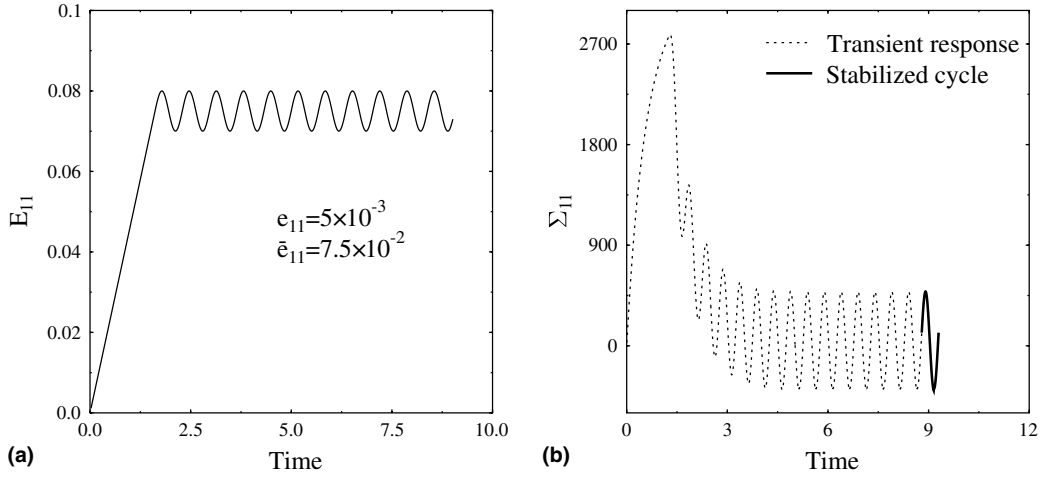


Fig. 1. (a) Macroscopic imposed strain and (b) stabilized cycle.

The effective harmonic shear modulus of the class of composites considered in this section can be expressed in closed-form by substituting $\hat{\mu}^{(2)}$, given by (35), into (33). This substitution gives

$$\tilde{\hat{\mu}}^{\mathrm{HS}}(p) = \tilde{\mu}^{A,\mathrm{HS}} p \frac{p + C}{(p + T_2^{-1})(p + T_c^{-1})}, \tag{39}$$

where $\tilde{\mu}^{A,\mathrm{HS}}$ is the Hashin–Shtrikman lower bound (33) for the composite effective instantaneous response, C a scalar, T_2 and T_c are two characteristic times defined as

$$\tilde{\mu}^{A,\mathrm{HS}} = \frac{\mu^{(2)}\mu^{(1)} + \mu^{(2)}(c_1\mu^{(1)} + c_2\mu^{(2)})}{\mu^{(2)} + c_2\mu^{(1)} + c_1\mu^{(2)}}, \qquad C = \frac{\mu^{(2)}\mu^{(1)}(c_1 + 1)}{\eta^{(2)}(\mu^{(1)}(1 + c_1) + c_2\mu^{(2)})},$$
$$T_2 = \frac{\eta^{(2)}}{\mu^{(2)}}, \qquad T_c = \frac{\eta^{(2)}(\mu^{(2)}(1 + c_1) + c_2\mu^{(1)})}{c_2\mu^{(2)}\mu^{(1)}}.$$

The effective harmonic shear modulus, as defined through (38), reads as

$$\tilde{\mu}^{\mathrm{HS}}(\omega) = |\tilde{\hat{\mu}}^{\mathrm{HS}}(\mathrm{i}\omega)|. \tag{40}$$

This relation gives the exact harmonic modulus of the composite which will serve as the reference for comparison purposes. It is identified as Laplace (HS) in Fig. 2.

The prediction of the present model is obtained by integrating in time the response of the model along the whole strain history until the macroscopic stress and strain reach (with a reasonable accuracy) a limit cycle called the stabilized cycle. The harmonic modulus estimated by the model is obtained from relation (38) where $\boldsymbol{e}$ and $\boldsymbol{s}$ refer to the stabilized cycle (see Fig. 1(b)). The harmonic shear modulus is then obtained as

$$\tilde{\mu}(\omega) = \frac{s_{\mathrm{eq}}}{3e_{\mathrm{eq}}} \quad \text{with } s_{\mathrm{eq}} = \sqrt{\frac{3}{2}\boldsymbol{s}^{\mathrm{d}} : \boldsymbol{s}^{\mathrm{d}}} \quad \text{and} \quad e_{\mathrm{eq}} = \sqrt{\frac{2}{3}\boldsymbol{e}^{\mathrm{d}} : \boldsymbol{e}^{\mathrm{d}}}. \tag{41}$$

The results shown in Fig. 2 for the present model correspond to a minus sign in relation (16). The effective energy of the thermoelastic problem have been estimated by the Hashin–Shtrikman lower bound (33). These results are identified as Model (HS). As can be seen in Fig. 2(a) the agreement between the exact result (40) and the predictions of the model is excellent at all frequencies.

4.2.2. Relaxation test

The same comparison can be made when the composite is subjected to a relaxation test. The load is again a shear strain (32) where the history of E_{11} is prescribed as

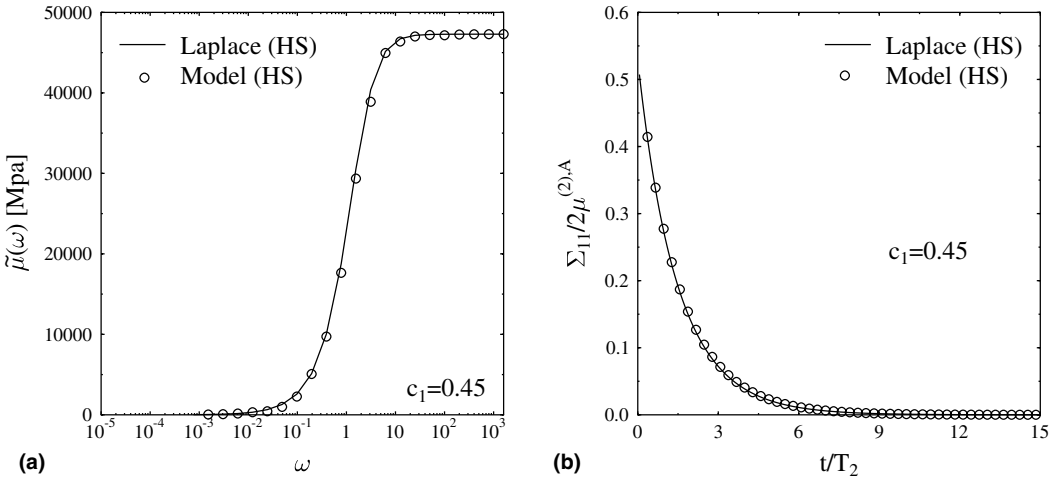


Fig. 2. Maxwell matrix isotropically reinforced by elastic fibers ($c_1 = 0.45$). Comparison between the present model (Model (HS)) and exact results (Laplace (HS)). (a) Cyclic loading, harmonic shear modulus $\tilde{\mu}(\omega)$ as a function of the driving frequency ω. (b) Relaxation test, effective stress normalized by the matrix instantaneous shear modulus $\mu^{(2),A}$, as a function of time normalized by $T_2 = \frac{\eta^{(2)}}{\mu^{(2)}}$.

$$\begin{aligned} E_{11}(t) &= 0 \quad \text{when } t < 0, \\ &= 1 \quad \text{when } t \geqslant 0. \end{aligned} \tag{42}$$

The Laplace transform of the strain history reads $\widehat{E_{11}}(p) = \frac{1}{p}$.

The exact response of the composite, identified as Laplace (HS), is obtained by applying the inverse Laplace transform to $\hat{\boldsymbol{\sigma}}(p)$

$$\boldsymbol{\Sigma}^{\mathrm{d}}(t) = \mathrm{L}^{-1}\left[2\hat{\tilde{\mu}}^{\mathrm{HS}}(p) : \widehat{\boldsymbol{E}}(p)\right] = \tilde{\mu}^{A,\mathrm{HS}}\left(b_1 \mathrm{e}^{-\frac{t}{T_2}} + b_2 \mathrm{e}^{-\frac{t}{T_c}}\right), \tag{43}$$

where

$$b_1 = \frac{T_2^{-1} - C}{T_2^{-1} - T_c^{-1}}, \qquad b_2 = \frac{C - T_c^{-1}}{T_2^{-1} - T_c^{-1}}.$$

The exact response and the prediction of the model for the effective stress, normalized by the instantaneous shear modulus of the matrix $\mu^{(2),A}$, are shown in Fig. 2(b) as a function of time normalized by $T_2 = \frac{\eta^{(2)}}{\mu^{(2)}}$. As in the case of cyclic loadings, the agreement of the model with the exact result is seen to be excellent.

4.3. Periodic microstructures

The composites under consideration in this section have a periodic microstructure consisting of identical circular fibers aligned with the x_3 axis and arranged at the nodes of a square lattice. A typical unit-cell is a square domain containing a circular fiber located at its center.

In the absence of exact relations for the effective properties of such composites, the accuracy of the proposed model is assessed by comparison with full numerical simulations by the finite element method of the response of this typical unit-cell subjected to prescribed loadings.

To evaluate separately the two types of error identified in Section 4.1, homogenization of the incremental viscoelastic problem and homogenization of the thermoelastic problem, four sets of results will be presented

1. The first set of results, identified as "Exact (FEM)" in the plots, is obtained by solving numerically (by the FEM) the viscoelastic local problem (4).

2. The second set of results, identified as "Model (FEM)", is obtained by approximating the incremental potential by the proposed scheme (lower bound corresponding to a minus sign in (16)), while the thermoelastic problem is solved exactly (by the FEM).
3. The third set of results, identified as "Model (HS)" is obtained by handling the incremental potential by the proposed model and by estimating the effective energy of the thermoelastic problem by an approximate scheme directly derived from the Hashin–Shtrikman procedure for periodic media (see Appendix A).
4. A fourth set of results, identified as "Model^{+} (FEM)", is obtained by approximating the incremental potential by the proposed scheme but with a sign plus in (16), while the thermoelastic problem is solved exactly (by the FEM). These results lie very far from the exact solution and, for this reason, are only shown for the first loading case.

The fibers (phase 1) are linear elastic and the surrounding matrix (phase 2) is viscoelastic. Two types of matrix have been considered:

- A Maxwell matrix (Table 1) characterized by the following material data:

$$2\mu^{(2)} = 53.84\ \text{GPa}, \qquad k^{(2)} = 58.33\ \text{GPa}, \qquad \eta^{(2)} = 10\ \text{GPa s}. \tag{44}$$

- A generalized Kelvin–Voigt matrix (Table 1) characterized by

$$\begin{aligned} 2\mu_1^{(2)} &= 53.84\ \text{GPa}, \qquad k_1^{(2)} = 58.33\ \text{GPa}, \\ 2\mu_2^{(2)} &= 26.92\ \text{GPa}, \qquad k_2^{(2)} = 29.16\ \text{GPa}, \qquad \eta^{(2)} = 10\ \text{GPa s}. \end{aligned} \tag{45}$$

Two types of inclusion were considered. The first case corresponds to fiber-reinforced composites and the material data for the fibers are $2\mu^{(1)} = 333.3$ GPa, $k^{(1)} = 222.2$ GPa. The second case corresponds to voided composites ($2\mu^{(1)} = k^{(1)} = 0$). The fiber volume-fraction ranges from $c_1 = 0.05$ to $c_1 = 0.5$.

The macroscopic strain are the purely deviatoric in-plane shear defined in (32). Two loading histories have been considered. The second history corresponds to (37).

4.3.1. Monotone loading

The first loading case is a monotonically increasing shear deformation with a constant macroscopic strain-rate $\dot{E}_{11}(t) = 5 \times 10^{-3}\ \text{s}^{-1}$.

4.3.1.1. Fiber-reinforced composites. The matrix considered in this section is a Maxwell material with characteristics given by (44). The main trends of the stress–strain curve of the composite under monotone deformation at constant strain-rate are typically an initial linear-elastic response for incipient strains, then a transient part which leads eventually to a plateau corresponding to the purely viscous response of the composite. This plateau is characterized by a stress Σ_{11}^{∞}. These trends are observed in Fig. 3 for the four sets of results exposed in Section 4.1 corresponding to the exact solution of the problem, to the sole approximation (15), lower and upper bounds, and to the approximation (15) coupled with the Hashin–Shtrikman estimate for periodic composites (A.8) of Appendix A. The Hashin–Shtrikman estimate is implemented with the matrix as the reference medium. Its prediction is therefore a lower bound for the effective stiffness and effective viscosity of the composite.

The following observations can be made:

1. The error due to the upper bound of the present model (approximation (15) with a + in the expression (16)), measured by the distance between the solid line and the square, is very large. This approximation will not be studied any more in the sequel.
2. The error due to the present model (approximation (15) with a − in the expression (16)), measured by the distance between the solid line and the crosses, is small (at least for the two volume fractions $c_1 = 0.25$ and $c_1 = 0.4$ which have been considered).

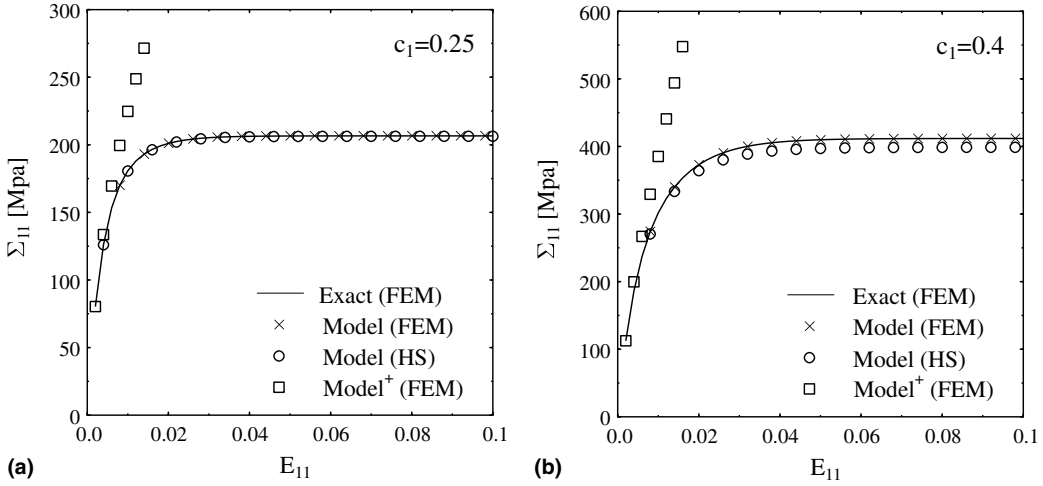


Fig. 3. Response of fiber-reinforced composites under monotone loading. Comparisons between the exact results (solid line), the present model, lower bound, with no approximation in the thermoelastic problem (×) and the present model coupled with the Hashin–Shtrikman approximation (○). The upper bound of the present model is also shown (□). (a) $c_1 = 0.25$, (b) $c_1 = 0.4$.

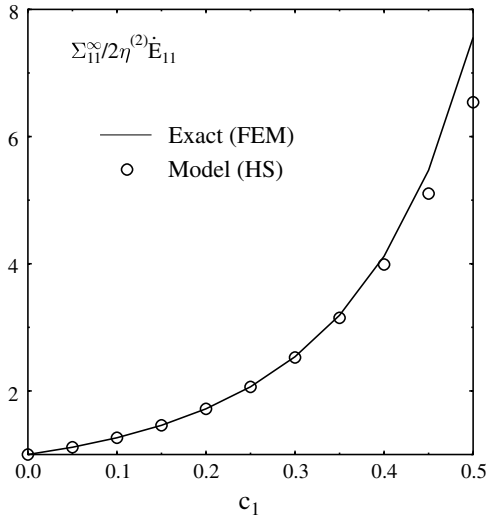


Fig. 4. Asymptotic stress Σ_{11}^{∞} as a function of the fiber volume-fraction. The asymptotic stress is normalized by the stress in the unreinforced matrix under the same loading conditions. Comparison between the exact result (solid line) and the Hashin–Shtrikman approximation (○).

3. The error due to the Hashin–Shtrikman approximation depends on the fiber volume-fraction. It is less than 1% when $c_1 = 0.25$, but is of the order of 3% when $c_1 = 0.4$. The maximal error is observed on the plateau.
4. The accuracy of the Hashin–Shtrikman approximation by itself can therefore be assessed by comparing its prediction for the asymptotic stress Σ_{11}^{∞} with exact FEM results. This comparison is performed in Fig. 4 as a function of the fiber volume-fraction c_1 ranging from 0 to 0.5. The asymptotic stress Σ_{11}^{∞} is normalized by $2\eta^{(2)}\dot{E}_{11}$ which is the stress in the pure matrix (with no reinforcement) under the same loading conditions.

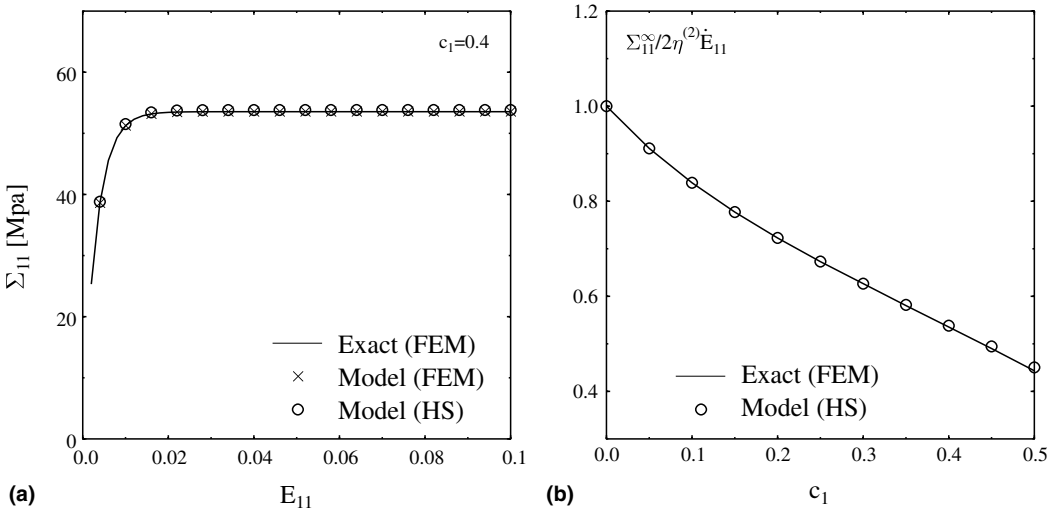


Fig. 5. Response of voided materials under monotone loading. Comparisons between the exact results (solid line), the present model with no approximation in the thermoelastic problem (×) and the present model coupled with the Hashin–Shtrikman approximation (○). (a) transient response for $c_1 = 0.4$. (b) Asymptotic stress Σ_{11}^{∞} as a function of the fiber volume-fraction. The asymptotic stress is normalized by the stress in the unreinforced matrix under the same loading conditions.

As expected, the Hashin–Shtrikman estimate is a lower bound for the actual asymptotic response of the composite.[3] However, it can be observed that the estimate deviates significantly from the exact results as the volume fraction increases. The error amounts to 13% when $c_1 = 0.5$. Use of the Hashin–Shtrikman approximation above $c_1 = 0.5$ would lead to large errors in the predictions.

4.3.1.2. Voided materials. A similar comparison can be made when the fibers are replaced by voids. The matrix is again a Maxwell material with material characteristics given by (44). The reference medium used in the Hashin–Shtrikman procedure is the matrix. The predictions of "Model (FEM)" and "Model (HS)" for the transient response of the composite are compared in Fig. 5(a) with the exact results "Exact (FEM)" for a void volume-fraction $c_1 = 0.4$. The agreement is seen to be excellent. A similar comparison is made for the asymptotic response of the composite (as t tends to $+\infty$) in Fig. 5(b). Again the agreement is excellent.

In conclusion the agreement of the proposed method with exact results is, for voided materials, very satisfactory, even in the approximate form of the model based on the Hashin–Shtrikman procedure.

4.3.2. Cyclic loadings

The cyclic loading (37) is applied to the unit-cell. The procedure adopted for the present model is described in Section 4.2.1. Two comparisons are made between the model and exact results: Fig. 6(a) and (b) shows the estimate of the effective harmonic modulus given by (38) as a function of the frequency ω for the Maxwell and the generalized Kelvin–Voigt matrix defined in (44) and (45). Fig. 6(c) presents the estimate of the effective stress for the stabilized cycle (defined in Fig. 1(b)) for a given frequency, $\omega = 6.25$ rad/s, as a function of time.

The estimate of the effective harmonic modulus given by "Model (HS)" is, at all frequencies, very close to the exact one for both the Maxwell and the generalized Kelvin–Voigt matrix. For the specific frequency $\omega = 6.25$ rad/s, the estimate of effective stress for the stabilized cycle given by "Model (HS)" is also in very good agreement with the exact results. The present model gives an accurate estimate of the phase shift between the macroscopic strain and the macroscopic stress (see Section 4.2.1).

[3] It is also a rigorous lower bound for the initial and the transient response of the composite.

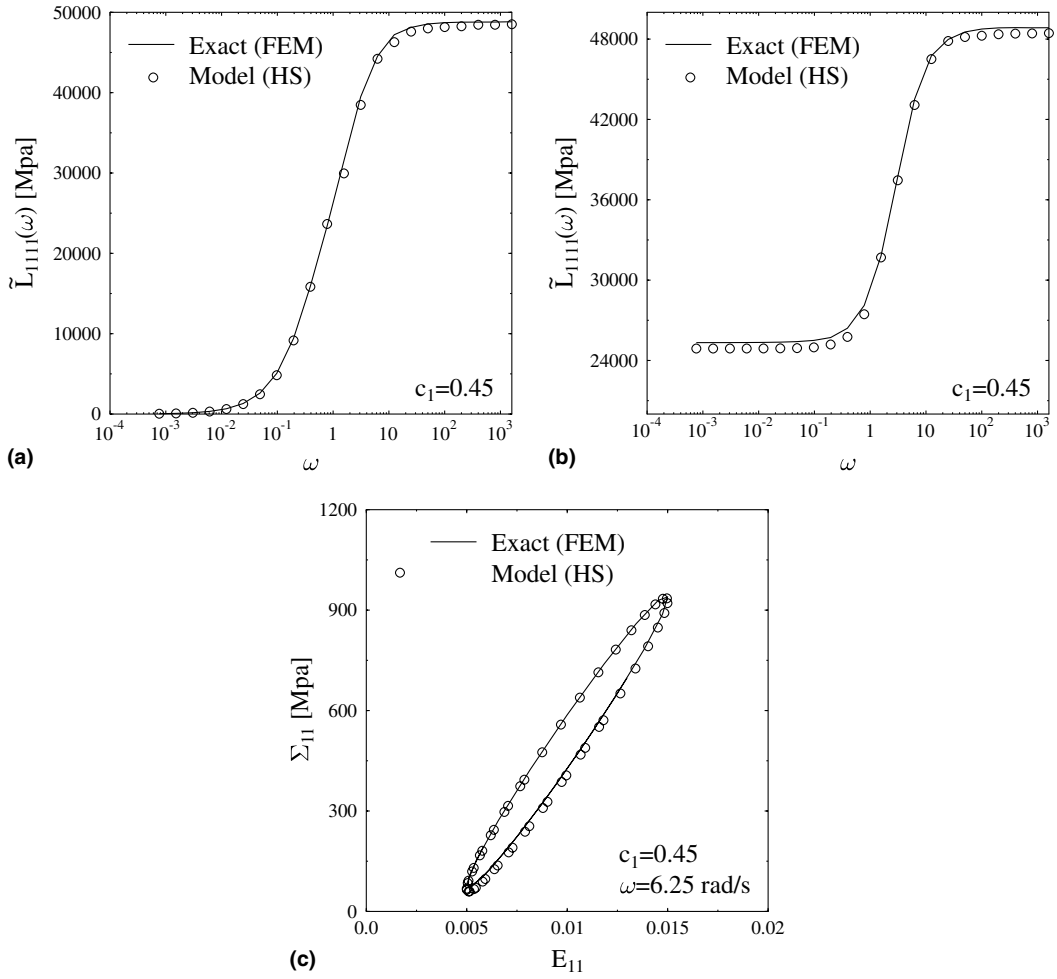


Fig. 6. Response of fiber-reinforced composites ($c_1 = 0.45$) under cyclic loading. Comparisons between the exact results (solid line) and the present model coupled with the Hashin–Shtrikman approximation (○). (a) $\tilde{L}_{1111}(\omega)$ estimate as a function of the frequency w for a Maxwell matrix. (b) $\tilde{L}_{1111}(\omega)$ estimate as a function of the frequency w for a generalized Kelvin–Voigt matrix. (c) Stabilized cycle for the generalized Kelvin–Voigt matrix with the frequency defined by $\omega = 6.25$ rad/s.

5. Conclusion

An approximate scheme for estimating the effective response of linear viscoelastic composites has been proposed. In contrast with most models in the literature based on the use of the Laplace transform, the proposed scheme operates directly in the time-domain by introducing an effective viscous strain (or effective internal variable) in each phase of the composite. The advantage of this procedure is twofold. First the resulting effective constitutive relations can easily be incorporated in a structural finite element code for computing the response of a viscoelastic composite structure to a macroscopic loading. Second, this procedure can be extended to nonlinear behaviors (on-going work).

The definition of this effective internal variable is performed in two steps.

- First, an incremental variational principle is derived to integrate in time the response of a composite material under a prescribed loading history.
- Second, a variational method directly inspired from the variational method of Ponte Castañeda (1992) is used to define the effective internal variable for each phase.

The predictions of the resulting approximate scheme are compared in Section 4 either with analytical results for specific microstructures or with full finite element simulations performed at the unit-cell level, both for inclusions stiffer than the surrounding matrix and for voids. The agreement is excellent both for monotone loadings and for cyclic loadings.

The proposed time-integration scheme can be used in conjunction with the Hashin–Shtrikman approximation for linear elastic composites. The accuracy of this second approximation is examined in the context of the present problem. It is shown that for fiber volume-fraction up to 0.4 the predictions of the method are not deteriorated by the HS approximation.

Appendix A. About the Hashin–Shtrikman estimates

This appendix recalls the expression of Hashin–Shtrikman estimates for periodic media and addresses the question of the determination of second-order moments of the strain field in the framework of this approximation.

A.1. The Hashin–Shtrikman procedure

For simplicity, attention is restricted here to linear-elastic composites (thermoelastic composites can be handled in an analogous way). Consider a N-phase linear-elastic composite where each individual phase is characterized by elastic moduli $\mathscr{L}^{(r)}$ which are uniform in the phase. The effective elastic energy of the composite is given by the variational property

$$\tilde{w}(\boldsymbol{E}) = \inf_{\boldsymbol{v}/\langle\boldsymbol{\epsilon}(\boldsymbol{v})\rangle=\boldsymbol{E}} \langle w^{(r)}(\boldsymbol{\varepsilon})\rangle, \tag{A.1}$$

where $\boldsymbol{\varepsilon} = \frac{1}{2}(\nabla\boldsymbol{v} + \nabla\boldsymbol{v}^{\mathrm{T}})$ and $w^{(r)}(\boldsymbol{\varepsilon}) = \frac{1}{2}\boldsymbol{\varepsilon} : \mathscr{L}^{(r)} : \boldsymbol{\varepsilon}$. The first step in the Hashin–Shtrikman procedure consists in adding and subtracting to the heterogeneous energy $w^{(r)}$, the energy $w^{(0)}$ of a homogeneous linear elastic medium with elastic moduli $\mathscr{L}^{(0)}$

$$w^{(0)}(\boldsymbol{\varepsilon}) = \frac{1}{2}\boldsymbol{\varepsilon} : \mathscr{L}^{(0)} : \boldsymbol{\varepsilon}.$$

Then, whenever $\mathscr{L}^{(r)} - \mathscr{L}^{(0)}$ is positive (respectively negative) in the sense of quadratic forms, $w^{(r)} - w^{(0)}$ is convex (resp. concave) and satisfies

$$(w^{(r)} - w^{(0)})(\boldsymbol{\varepsilon}) = \sup_{\boldsymbol{s}} \left(\boldsymbol{s} : \boldsymbol{\varepsilon} - (w^{(r)} - w^{(0)})^*(\boldsymbol{s})\right),$$

where $(w^{(r)} - w^{(0)})^*$ is the convex dual (resp. concave) of $w^{(r)} - w^{(0)}$.[4] Therefore

$$\tilde{w}(\boldsymbol{E}) = \inf_{\boldsymbol{v}} \sup_{\boldsymbol{s}} \langle w^{(0)}(\boldsymbol{\varepsilon}) + \boldsymbol{s} : \boldsymbol{\varepsilon}\rangle - \left\langle (w^{(r)} - w^{(0)})^*(\boldsymbol{s})\right\rangle. \tag{A.2}$$

The dual of $w^{(r)} - w^{(0)}$ can be computed as

$$(w^{(r)} - w^{(0)})^*(\boldsymbol{s}) = \inf_{\boldsymbol{\epsilon}} \left[\boldsymbol{\varepsilon} : \boldsymbol{s} - \frac{1}{2}\boldsymbol{\varepsilon} : (\mathscr{L}^{(r)} - \mathscr{L}^{(0)}) : \boldsymbol{\varepsilon}\right]. \tag{A.3}$$

Resolving the infimum for $\boldsymbol{\varepsilon}$ yields

$$\boldsymbol{\varepsilon} = (\mathscr{L}^{(r)} - \mathscr{L}^{(0)})^{-1} : \boldsymbol{s}, \tag{A.4}$$

which gives

$$(w^{(r)} - w^{(0)})^*(\boldsymbol{s}) = \frac{1}{2}\boldsymbol{s} : (\mathscr{L}^{(r)} - \mathscr{L}^{(0)})^{-1} : \boldsymbol{s}. \tag{A.5}$$

[4] It is assumed in the sequel that $\mathscr{L}^{(r)} - \mathscr{L}^{(0)}$ is positive. The opposite case where $\mathscr{L}^{(r)} - \mathscr{L}^{(0)}$ is negative can be handled in the same way upon exchange of inf and sup. The resulting bound would be an upper bound.

Upon substitution of this expression in (A.2) we obtain

$$\tilde{w}(\boldsymbol{E}) = \operatorname*{Inf}_{\boldsymbol{v}} \operatorname*{Sup}_{\boldsymbol{s}} \left[\langle w^{(0)}(\boldsymbol{\varepsilon}) + \boldsymbol{s} : \boldsymbol{\varepsilon} \rangle - \left\langle \frac{1}{2} \boldsymbol{s} : (\mathscr{L}^{(r)} - \mathscr{L}^{(0)})^{-1} : \boldsymbol{s} \right\rangle \right]. \tag{A.6}$$

The next step in the Hashin–Shtrikman procedure is to limit attention to polarization fields $\boldsymbol{s}$ which are uniform in each individual phase

$$\boldsymbol{s}(\boldsymbol{x}) = \sum_{r=1}^{N} \boldsymbol{s}^{(r)} \chi^{(r)}(\boldsymbol{x}).$$

Then the following lower bound is obtained:

$$\begin{aligned} \tilde{w}(\boldsymbol{E}) \geqslant \mathscr{HS}(\mathscr{L}^{(r)}|_{r=1,\ldots,N}, \mathscr{L}^{(0)}, \boldsymbol{E}) \stackrel{\text{def}}{=} \operatorname*{Inf}_{\boldsymbol{v}} \\ \times \operatorname*{Sup}_{\boldsymbol{s}^{(r)}} \left[\langle w^{(0)}(\boldsymbol{\varepsilon}) + \boldsymbol{s}^{(r)} : \boldsymbol{\varepsilon} \rangle - \left\langle \frac{1}{2} \boldsymbol{s}^{(r)} : (\mathscr{L}^{(r)} - \mathscr{L}^{(0)})^{-1} : \boldsymbol{s}^{(r)} \right\rangle \right]. \end{aligned} \tag{A.7}$$

When one of the phases, say phase N, is weaker than the other phases, the best lower bound given by (A.7) is obtained by taking $\mathscr{L}^{(0)} = \mathscr{L}^{(N)}$. The resulting expression is *the Hashin–Shtrikman lower bound*

$$\tilde{w}(\boldsymbol{E}) \geqslant \tilde{w}^{\mathrm{HS}}(\boldsymbol{E}), \quad \text{where } \tilde{w}^{\mathrm{HS}}(\boldsymbol{E}) = \mathscr{HS}(\mathscr{L}^{(r)}|_{r=1,\ldots,N}, \mathscr{L}^{(N)}, \boldsymbol{E}). \tag{A.8}$$

The general expressions (A.7) and (A.8) can be further simplified (see below), but they are sufficient for the derivation of the second-order moment of the strain in each individual phase, in the context of the Hashin–Shtrikman procedure.

A.2. Second moments and the Hashin–Shtrikman approximation

As is well-known (see for instance Kreher and Pompe, 1985; Ponte Castañeda and Suquet, 1998) the second-order moment of the strain field in each phase of the initial thermoelastic composite reads

$$\langle \boldsymbol{\varepsilon} \otimes \boldsymbol{\varepsilon} \rangle_r = \frac{2}{c^{(r)}} \frac{\partial \tilde{w}}{\partial \mathscr{L}^{(r)}}(\boldsymbol{E}). \tag{A.9}$$

This subsection examines how this relation is modified when the Hashin–Shtrikman bound $\tilde{w}^{\mathrm{HS}}$ is substituted to $\tilde{w}$.

First, the partial derivatives of $\tilde{w}^{\mathrm{HS}}$ and $\mathscr{HS}$ are related by

$$\frac{\partial \tilde{w}^{\mathrm{HS}}}{\partial \mathscr{L}^{(r)}}(\boldsymbol{E}) = \frac{\partial \mathscr{HS}}{\partial \mathscr{L}^{(r)}}(\mathscr{L}^{(r)}|_{r=1,\ldots,N}, \mathscr{L}^{(N)}, \boldsymbol{E}) \quad \text{when } 1 \leqslant r \leqslant N-1, \tag{A.10}$$

$$\frac{\partial \tilde{w}^{\mathrm{HS}}}{\partial \mathscr{L}^{(N)}}(\boldsymbol{E}) = \left(\frac{\partial \mathscr{HS}}{\partial \mathscr{L}^{(N)}} + \frac{\partial \mathscr{HS}}{\partial \mathscr{L}^{(0)}} \right)(\mathscr{L}^{(r)}|_{r=1,\ldots,N}, \mathscr{L}^{(N)}, \boldsymbol{E}). \tag{A.11}$$

Then, it follows from (A.7) that

$$\frac{\partial \mathscr{HS}}{\partial \mathscr{L}^{(r)}} = -\frac{c^{(r)}}{2} \boldsymbol{s}^{(r)} : \frac{\partial (\mathscr{L}^{(r)} - \mathscr{L}^{(0)})^{-1}}{\partial \mathscr{L}^{(r)}} : \boldsymbol{s}^{(r)}, \tag{A.12}$$

$$\frac{\partial \mathscr{HS}}{\partial \mathscr{L}^{(0)}} = \frac{1}{2} \langle \boldsymbol{\varepsilon} \otimes \boldsymbol{\varepsilon} \rangle - \sum_{r=1}^{N} \frac{c^{(r)}}{2} \boldsymbol{s}^{(r)} : \frac{\partial (\mathscr{L}^{(r)} - \mathscr{L}^{(0)})^{-1}}{\partial \mathscr{L}^{(0)}} : \boldsymbol{s}^{(r)}. \tag{A.13}$$

Note first that

$$\frac{\partial (\mathscr{L}^{(r)} - \mathscr{L}^{(0)})^{-1}}{\partial \mathscr{L}^{(r)}} = -\frac{\partial (\mathscr{L}^{(r)} - \mathscr{L}^{(0)})^{-1}}{\partial \mathscr{L}^{(0)}} = -(\mathscr{L}^{(r)} - \mathscr{L}^{(0)})^{-1} \otimes (\mathscr{L}^{(r)} - \mathscr{L}^{(0)})^{-1}.$$

It follows from the optimality condition with respect to $\boldsymbol{s}^{(r)}$ in (A.7) that

$$\boldsymbol{s}^{(r)} = (\mathscr{L}^{(r)} - \mathscr{L}^{(0)}) : \langle \varepsilon \rangle_r. \tag{A.14}$$

Then, reporting these relations in (A.11) and (A.13) one obtains

$$\begin{aligned}\frac{\partial \tilde{w}^{\mathsf{HS}}}{\partial \mathscr{L}^{(r)}}(\boldsymbol{E}) &= \frac{c^{(r)}}{2}\langle \boldsymbol{\varepsilon} \rangle_r \otimes \langle \boldsymbol{\varepsilon} \rangle_r \quad \text{when } 1 \leqslant r \leqslant N-1 \\ &= \frac{c^{(r)}}{2}\left(\langle \boldsymbol{\varepsilon} \otimes \boldsymbol{\varepsilon} \rangle_r - \langle (\boldsymbol{\varepsilon} - \langle \boldsymbol{\varepsilon} \rangle_r) \otimes (\boldsymbol{\varepsilon} - \langle \boldsymbol{\varepsilon} \rangle_r) \rangle_r\right), \end{aligned} \tag{A.15}$$

$$\begin{aligned}\frac{\partial \tilde{w}^{\mathsf{HS}}}{\partial \mathscr{L}^{(N)}}(\boldsymbol{E}) &= \frac{1}{2}\langle \boldsymbol{\varepsilon} \otimes \boldsymbol{\varepsilon} \rangle - \sum_{r=1}^{N-1} \frac{c^{(r)}}{2}\langle \boldsymbol{\varepsilon} \rangle_r \otimes \langle \boldsymbol{\varepsilon} \rangle_r \\ &= \frac{c^{(N)}}{2}\langle \boldsymbol{\varepsilon} \otimes \boldsymbol{\varepsilon} \rangle_N + \sum_{r=1}^{N-1} \frac{c^{(r)}}{2}\langle (\boldsymbol{\varepsilon} - \langle \boldsymbol{\varepsilon} \rangle_r) \otimes (\boldsymbol{\varepsilon} - \langle \boldsymbol{\varepsilon} \rangle_r) \rangle_r, \end{aligned} \tag{A.16}$$

where now $\boldsymbol{\varepsilon}$ is the strain field in the homogeneous linear elastic body with stiffness $\mathscr{L}^{(0)} = \mathscr{L}^{(N)}$. In other words, relation (A.9) holds only with the exact effective energy $\tilde{w}$. When one replaces the exact effective energy by the Hashin–Shtrikman energy, the derivatives of the energy with respect to the moduli overestimates the second moment in the phase which is taken as the reference medium and underestimates these moments in the other phases. The only exception occurs when the fluctuations of the strain field inside the $N-1$ phases other than the phase taken as the reference medium vanish identically. This can be achieved in specific microstructures for which the Hashin–Shtrikman estimate is exact, but is not true in other situations. In particular it is not true in periodic media where the Hashin–Shtrikman procedure delivers only an approximation (and a bound) for the effective properties. The error made in using relations (A.9) with the Hashin–Shtrikman approximation is discussed in more details in Section A.4.

A.3. Hashin–Shtrikman bounds and estimates for periodic media

The Euler–Lagrange equations for the infimum problem

$$\inf_{\boldsymbol{v}} \langle w^{(0)}(\boldsymbol{\varepsilon}) + \boldsymbol{s}^{(r)} : \boldsymbol{\varepsilon} \rangle, \tag{A.17}$$

read as

$$\operatorname{div}\boldsymbol{\sigma} = \boldsymbol{0}, \quad \boldsymbol{\sigma} = \mathscr{L}^{(0)} : \boldsymbol{\varepsilon} + \boldsymbol{s}^{(r)}, \quad \text{and} \quad \langle \boldsymbol{\varepsilon} \rangle = \boldsymbol{E}. \tag{A.18}$$

The solution of (A.18) can be expressed by means of the Green operator associated with $\mathscr{L}^{(0)}$. For an arbitrary polarization field $\boldsymbol{\theta}(\boldsymbol{x})$, $\boldsymbol{\Gamma}^{(0)} \bigstar \boldsymbol{\theta}$ is by definition the strain field $\boldsymbol{\varepsilon}^*$ solution of

$$\operatorname{div}\boldsymbol{\sigma} = \boldsymbol{0}, \quad \text{with } \boldsymbol{\sigma} = \mathscr{L}^{(0)} : \boldsymbol{\varepsilon}^* - \boldsymbol{\theta}, \quad \text{and} \quad \langle \boldsymbol{\varepsilon}^* \rangle = \boldsymbol{0}. \tag{A.19}$$

Then the solution of (A.18) can be written as

$$\boldsymbol{\varepsilon}(\boldsymbol{x}) = \boldsymbol{\varepsilon}^*(\boldsymbol{x}) + \boldsymbol{E}, \quad \text{with } \boldsymbol{\varepsilon}^*(\boldsymbol{x}) = -\sum_{r=1}^{N} \boldsymbol{\Gamma}^{(0)} \bigstar \chi^{(r)}(\boldsymbol{x}) : \boldsymbol{s}^{(r)}. \tag{A.20}$$

After straightforward algebra, the infimum in (A.17) reduces to

$$w^{(0)}(\boldsymbol{E}) + \sum_{r=1}^{N} c^{(r)} \boldsymbol{s}^{(r)} : \boldsymbol{E} - \frac{1}{2}\sum_{r,s=1}^{N} \boldsymbol{s}^{(r)} : \boldsymbol{\Gamma}^{(rs)} : \boldsymbol{s}^{(s)}, \tag{A.21}$$

where

$$\boldsymbol{\Gamma}^{(rs)} = \langle \chi^{(r)} \boldsymbol{\Gamma}^{(0)} \bigstar \chi^{(s)} \rangle.$$

The resulting expression for the Hashin–Shtrikman functional is

$$\mathscr{HS}(\mathscr{L}^{(r)},\mathscr{L}^{(0)},\boldsymbol{E}) = \sup_{\boldsymbol{s}^{(r)}}\left[w^{(0)}(\boldsymbol{E}) + \sum_{r=1}^{N} c^{(r)}\boldsymbol{s}^{(r)} : \boldsymbol{E} - \frac{1}{2}\sum_{r,s=1}^{N}\boldsymbol{s}^{(r)} : \boldsymbol{\Gamma}^{(rs)} : \boldsymbol{s}^{(s)} - \frac{1}{2}\sum_{r=1}^{N} c^{(r)}\boldsymbol{s}^{(r)} : (\mathscr{L}^{(r)} - \mathscr{L}^{(0)})^{-1} : \boldsymbol{s}^{(r)}\right]. \tag{A.22}$$

The optimality conditions with respect to $\boldsymbol{s}^{(r)}$ read

$$\sum_{s=1}^{N}\left[c^{(s)}\delta_{rs}(\mathscr{L}^{(s)} - \mathscr{L}^{(0)})^{-1} + \boldsymbol{\Gamma}^{(rs)}\right] : \boldsymbol{s}^{(s)} = c^{(r)}\boldsymbol{E}, \quad r = 1,\ldots,N. \tag{A.23}$$

Substitution of the solutions of these equations into (A.22) gives the final form of the Hashin–Shtrikman functional.

Specific expressions for $\boldsymbol{\Gamma}^{(rs)}$ have been obtained in the case of periodic media by Nemat-Nasser et al. (1982), Milton and Kohn (1988) and Suquet (1990). Let $\mathscr{R}$ denote the original discrete periodic lattice and $\mathscr{R}^*$ its reciprocal lattice. First, it can be shown that the Fourier transform of $\boldsymbol{\Gamma}^{(0)}$ at frequency $\boldsymbol{\xi} \neq \boldsymbol{0}$[5] reads as

$$\widehat{\boldsymbol{\Gamma}}^{(0)}(\boldsymbol{\xi}) = \boldsymbol{\xi}\otimes\boldsymbol{N}^{(0)}(\boldsymbol{\xi})\otimes\boldsymbol{\xi}|_{\mathrm{sym}}, \quad \boldsymbol{N}^{(0)}(\boldsymbol{\xi}) = (\boldsymbol{K}^{(0)}(\boldsymbol{\xi}))^{-1}, \quad \boldsymbol{K}^{(0)}(\boldsymbol{\xi}) = \boldsymbol{\xi}\cdot\mathscr{L}^{(0)}\cdot\boldsymbol{\xi}.$$

Then the Fourier transform of the field $\boldsymbol{\Gamma}^{(0)} \bigstar \boldsymbol{\theta}$ is $\widehat{\boldsymbol{\Gamma}}^{(0)}(\boldsymbol{\xi}) : \hat{\boldsymbol{\theta}}(\boldsymbol{\xi})$. Then, using Plancherel's theorem, one obtains that

$$\boldsymbol{\Gamma}^{(rs)} = \sum_{\boldsymbol{\xi}\in\mathscr{R}^*}\hat{\chi}^{(r)}(-\boldsymbol{\xi})\widehat{\boldsymbol{\Gamma}}^{(0)}(\boldsymbol{\xi})\hat{\chi}^{(s)}(\boldsymbol{\xi}). \tag{A.24}$$

Comments:

(1) The tensors $\boldsymbol{\Gamma}^{(rs)}$ are not independent and satisfy in particular the relations

$$\sum_{s=1}^{N}\boldsymbol{\Gamma}^{(rs)} = 0, \qquad \sum_{r=1}^{N}\boldsymbol{\Gamma}^{(rs)} = 0, \qquad \boldsymbol{\Gamma}^{(rs)} = \boldsymbol{\Gamma}^{(sr)}.$$

The first relation follows from the fact that a uniform polarization field induces no strain in a uniform medium, the second relation comes from the fact that $\boldsymbol{\Gamma}^{0}$ is a projector on fields whose average is equal to 0 and the third relation is a consequence of the symmetries of $\mathscr{L}^{(0)}$.

(2) In particular, the tensors $\boldsymbol{\Gamma}^{(rs)}$ for two-phase materials satisfy the relations

$$\boldsymbol{\Gamma}^{(11)} + \boldsymbol{\Gamma}^{(12)} = 0, \qquad \boldsymbol{\Gamma}^{(21)} + \boldsymbol{\Gamma}^{(22)} = 0.$$

Therefore, they can all be expressed in terms of a single tensor $\mathbf{P}$ as

$$\boldsymbol{\Gamma}^{(rs)} = c^{(r)}(\delta_{rs} - c^{(s)})\boldsymbol{P}, \quad \text{where } \boldsymbol{P} = \frac{1}{c^{(1)}c^{(2)}}\boldsymbol{\Gamma}^{(11)}. \tag{A.25}$$

For two-phase composite the system (A.23) reads as

$$[c^{(1)}(\mathscr{L}^{(1)} - \mathscr{L}^{(2)})^{-1} + \boldsymbol{\Gamma}^{(11)}] : \boldsymbol{s}^{(1)} = c^{(1)}\boldsymbol{E}, \qquad \boldsymbol{s}^{(2)} = \boldsymbol{0}.$$

It follows from these equations and from relation (A.25) that

$$\boldsymbol{s}^{(1)} = [(\mathscr{L}^{(1)} - \mathscr{L}^{(2)})^{-1} + c^{(2)}\boldsymbol{P}]^{-1} : \boldsymbol{E}, \qquad \boldsymbol{s}^{(2)} = \boldsymbol{0}, \tag{A.26}$$

and from relations (A.14) and (29) that

$$\boldsymbol{A}^{(1)} = [\boldsymbol{I} + c^{(2)}\boldsymbol{P} : (\mathscr{L}^{(1)} - \mathscr{L}^{(2)})]^{-1}, \qquad \boldsymbol{a}^{(1)} = -c^{(2)}\boldsymbol{A}^{(1)} : \boldsymbol{P} : (\boldsymbol{\tau}^{(1)} - \boldsymbol{\tau}^{(2)}). \tag{A.27}$$

[5] Since $\langle\varepsilon^*\rangle = \boldsymbol{0}$, one can set $\widehat{\boldsymbol{\Gamma}}^{(0)}(\boldsymbol{0}) = \boldsymbol{0}$.

Finally, substituting (A.26) in (A.22) with $\mathscr{L}^{(0)} = \mathscr{L}^{(2)}$, one obtains

$$\tilde{w}^{\mathrm{HS}}(\boldsymbol{E}) = w^{(2)}(\boldsymbol{E}) + \frac{1}{2}c^{(1)}\boldsymbol{s}^{(1)} : \boldsymbol{E} = \frac{1}{2}\boldsymbol{E} : \widetilde{\mathscr{L}} : \boldsymbol{E},$$

with

$$\widetilde{\mathscr{L}}^{\mathrm{HS}} = \mathscr{L}^{(2)} + c_1(\mathscr{L}^{(1)} - \mathscr{L}^{(2)}) : \boldsymbol{A}^{(1)}. \tag{A.28}$$

(3) When the reference medium is isotropic and characterized by Lamé coefficients $\lambda^{(0)}$ and $\mu^{(0)}$, the Fourier transform of $\boldsymbol{\Gamma}^{(0)}$ reduces to

$$\widehat{\Gamma}^{(0)}_{ijkh} = \frac{1}{\mu^{(0)}}\left(\frac{\delta_{ki}\xi_h\xi_j + \delta_{hi}\xi_k\xi_j + \delta_{kj}\xi_h\xi_i + \delta_{hj}\xi_k\xi_i}{4|\boldsymbol{\xi}|^2} - \frac{\lambda^0 + \mu^0}{\lambda^0 + 2\mu^0}\frac{\xi_i\xi_j\xi_k\xi_h}{|\boldsymbol{\xi}|^4}\right).$$

(4) When phase 1 is a circular fiber with radius a centered at the origin and parallel to the third direction, the Fourier transform of its characteristic function reads

$$\hat{\chi}^{(1)}(\boldsymbol{\xi}) = c^{(1)}\frac{2J_1(ak)}{ak} \quad \text{where } k = (\xi_1^2 + \xi_2^2)^{1/2},$$

and J_1 is the Bessel function of the first kind and of order 1.

A.4. Comparison of predictions for the second-order moments in two-phase periodic composites

Consider a two-phase periodic composite comprised of hard fibers (phase 1) in a matrix (phase 2) satisfying $\mathscr{L}^{(1)} \geqslant \mathscr{L}^{(2)}$ in the sense of quadratic forms. This section compares several predictions for the second moment of the strain field in the matrix as a function of the fiber/matrix contrast. More specifically the composite is comprised of isotropic phases and we are interested in the quantity $\langle \boldsymbol{\varepsilon}^{\mathrm{d}} : \boldsymbol{\varepsilon}^{\mathrm{d}} \rangle_2$, (where $\boldsymbol{\varepsilon}^{\mathrm{d}}$ stands for the deviator of $\boldsymbol{\varepsilon}$) which is an isotropic invariant of the second moment of the strain in the matrix.

This invariant can be computed exactly (up to numerical errors) by solving numerically the inhomogeneous elasticity problem. The corresponding prediction will be labelled as "FEM" in Fig. A.1. It can also be approximated by the second moment in the matrix of the strain field solution of (A.18). This can be done in two dif-

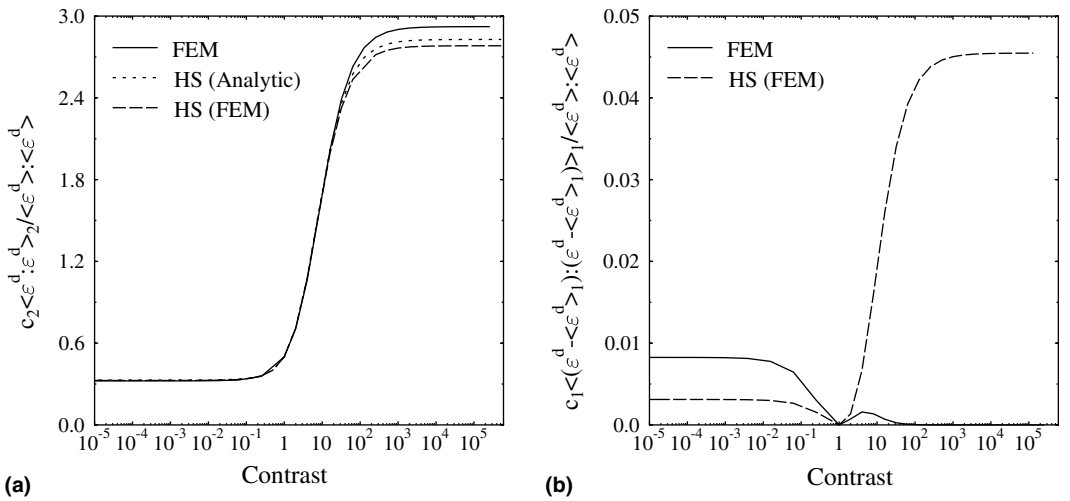


Fig. A.1. Circular fibers arranged at the nodes of a square lattice. Fiber volume fraction $c_1 = 0.5$ (a) second moment of the strain field in the matrix phase. (b) fluctuations of the strain field in the inclusion. Comparison between: The exact results, corresponding to the solution of the initial problem (A.1) obtained by the finite element method, denoted FEM. Exact solution of the homogenized problem (A.8), denoted HS (FEM). Approximation given by formula (A.30) obtained by neglecting the fluctuations in the inclusion, denoted HS (Analytic).

ferent ways. First, the exact second moment of the exact solution of (A.18) can be computed by the FEM. The corresponding predictions are labelled "HS (FEM)" in Fig. A.1. Second relation (A.9) can be applied to the Hashin–Shtrikman approximate energy by using the approximate relation

$$\langle \boldsymbol{\varepsilon}^{\mathrm{d}} : \boldsymbol{\varepsilon}^{\mathrm{d}} \rangle_2 \simeq \frac{1}{c^{(2)}} \frac{\partial \tilde{w}^{\mathrm{HS}}}{\partial \mu^{(2)}}, \tag{A.29}$$

$\tilde{w}^{\mathrm{HS}}$ being computed with expression (A.8). The corresponding predictions are labelled "HS (Analytic)" in Fig. A.1.

As pointed out in section (A.2), the third method overestimates the quantity of interest since

$$\frac{\partial \tilde{w}^{\mathrm{HS}}}{\partial \mu^{(2)}} = c^{(2)} \langle \boldsymbol{\varepsilon}^{\mathrm{d}} : \boldsymbol{\varepsilon}^{\mathrm{d}} \rangle_2 + c^{(1)} \langle (\boldsymbol{\varepsilon}^{\mathrm{d}} - \langle \boldsymbol{\varepsilon}^{\mathrm{d}} \rangle_1) : (\boldsymbol{\varepsilon}^{\mathrm{d}} - \langle \boldsymbol{\varepsilon}^{\mathrm{d}} \rangle_1) \rangle_1. \tag{A.30}$$

The unit-cell is a square containing a circular fiber located at its center. All calculations are performed in plane strain. The applied deformation is an in-plane shear in the form (32). The elastic properties in the matrix are chosen proportional to that of the matrix with a proportionality ratio defining the contrast between the phases (in terms of the Young modulus and Poisson ratio, these relations are $E^{(1)} = \text{contrast} \times E^{(2)}$, $\nu^{(1)} = \nu^{(2)}$).

It can be observed in Fig. A.1(a) that when the contrast between the phases is moderate, less than 10, the three predictions are in very good agreement. For moderate constrast, the Hashin–Shtrikman effective energy and the approximate relation (A.29) can legitimately be used to compute the second moment of the strain in the matrix. In agreement with this observation, the fluctuations of the strain field in the inclusions, shown in Fig. A.1(b) are seen to be reasonably small and can be neglected in (A.30).

For larger contrast, the Hashin–Shtrikman approximation HS (FEM) underestimates the second moment in the matrix (the error is of the order of 5% at most in the present configuration and loading conditions). This underestimation is partly compensated in the third method (labelled HS (Analytic)) which neglects the fluctuations in the inclusions. The compensation of the two errors brings an improvement to the predictions of the third method which are seen to be closer to the actual results than that obtained by the second method.

In conclusion, the error introduced by the relation (A.29) remains limited in the microstructure under consideration for the range of contrast which have been considered in the rest of this study. Therefore this relation can been used here as a satisfactory approximation of the second-moment of the strain field in the matrix.

References

Barbero, E., Luciano, R., 1995. Micromechanical formulas for the relaxation tensor of linear viscoelastic composites with transversely isotropic fibers. Int. J. Solids Struct. 32, 1859–1872.

Brenner, R., Masson, R., Castelnau, O., Zaoui, A., 2002. A "quasi-elastic" affine formulation for the homogenised behaviour of nonlinear viscoelastic polycrystals and composites. Eur. J. Mech.—A/Solids 21, 943–960.

Brenner, R., Masson, R., 2005. Improved affine estimates for nonlinear viscoelastic composites. Eur. J. Mech.—A/Solids 24, 1002–1015.

Brinson, L.C., Lin, W.S., 1998. Comparison of micromechanics methods for effective properties of multiphase viscoelastic composites. Compos. Struct. 41, 353–367.

Chabert, E., Bornert, M., Bourgeat-Lami, E., Cavaille, J.Y., Dendievel, R., Gauthier, C., Putaux, J.L., Zaoui, A., 2004. Filler–filler interactions and viscoelastic behavior of polymer nanocomposites. Mater. Sci. Eng. A 381, 320–330.

DeBotton, G., Tevet-Deree, L., 2004. The response of a fiber-reinforced composite with a viscoelastic matrix phase. J. Compos. Mater. 38, 1255–1277.

Francfort, G., Murat, F., 1986. Homogenization and optimal bounds in linear elasticity. Arch. Ration. Mech. Anal. 94, 307–334.

Gibiansky, L., Milton, G., Berryman, J., 1999. On the effective viscoelastic moduli of two-phase media: III. rigourous bounds on the complex shear modulus in two dimensions. Proc. Roy. Soc. Lond. A 455, 2117–2149.

Hashin, Z., 1970. Complex moduli of viscoelastic composites—I. General theory and application to particulate composites. Int. J. Solids Struct. 6, 539–552.

Houshyar, S., Shanks, R., Hodzic, A., 2005. Tensile creep behaviour of polypropylene fibre reinforced polypropylene composites. Polym. Test. 24, 257–264.

Kreher, W., Pompe, W., 1985. Field fluctuations in a heterogeneous elastic material—an information theory approach. J. Mech. Phys. Solids 33, 419–445.

Lahellec, N., Suquet, P., 2003. Composites non linéaires à deux potentiels: esti- mations affine et du second-order. In: Potier-Ferry, M., Bonnet, M., Bignon- net, A. (Eds.), 6ème Colloque National en Calcul des Structures. Tome 3. CSMA, 49-56.

Laws, N., Mc Laughlin, R., 1978. Self-consistent estimates for the viscoelastic creep compliance of composite materials. Proc. Roy. Soc. Lond. A 359, 251–273.

Levin, V., 1967. Thermal expansion coefficients of heterogeneous materials. Mekh. Tverd. Tela 2, 83–94.
Masson, R., Zaoui, A., 1999. Self-consistent estimates for the rate-dependent elastoplastic behaviour of polycrystalline materials. J. Mech. Phys. Solids 47, 1543–1568.
Milton, G., Kohn, R., 1988. Variational bounds of the effective moduli of anisotropic composites. J. Mech. Phys. Solids 36, 597–629.
Nemat-Nasser, S., Iwakuma, I., Hejazi, M., 1982. On composites with periodic microstructure. Mech. Mater. 1, 239–267.
Papanicolaou, G., Zaoutsos, S., Kontou, E., 1999. Prediction of the non-linear viscoelastic response of unidirectional fiber composites. Compos. Sci. Technol. 59, 1311–1319.
Ponte Castañeda, P., 1992. New variational principles in plasticity and their application to composite materials. J. Mech. Phys. Solids 40, 1757–1788.
Ponte Castañeda, P., 2002. Second-order homogenization estimates for nonlinear composites incorporating field fluctuations. I—Theory. J. Mech. Phys. Solids 50, 737–757.
Ponte Castañeda, P., Suquet, P., 1998. Nonlinear composites. Adv. Appl. Mech. 34, 171–302.
Ponte Castañeda, P., Willis, J.R., 1999. Variational second-order estimates for nonlinear composites. Proc. Roy. Soc. Lond. A 455, 1799–1811.
Rougier, Y., Stolz, C., Zaoui, A., 1993. Représentation spectrale en viscoélasticité linéaire des matériaux hétérogènes. CR Acad. Sci. Paris IIb 316, 1517–1522.
Sanchez-Hubert, J., Sanchez-Palencia, E., 1978. Sur certains problèmes physiques d'homogénéisation donnant lieu à des phénomènes de relaxation. CR Acad. Sci. Paris A 286, 903–906.
Suquet, P., 1986. Elements of homogenization for inelastic solid mechanics. In: Sanchez-Palencia, E., Zaoui, A. (Eds.), Homogenization Techniques for Composite Media, Lecture Notes in Physics, vol. 272. Springer-Verlag, Berlin, pp. 193–278.
Suquet, P., 1990. Une méthode simplifiée pour le calcul des propriétés élastiques de matériaux hétérogènes à structure périodique. CR Acad. Sci. Paris IIb 311, 769–774.
Suquet, P., 1995. Overall properties of nonlinear composites: a modified secant moduli theory and its link with Ponte Castañeda's nonlinear variational procedure. CR Acad. Sci. Paris IIb 320, 563–571.
Vinogradov, V., Milton, G., 2005. The total creep of viscoelastic composites under hydrostatic or antiplane loading. J. Mech. Phys. Solids 53, 1248–1279.
Willis, J., 1981. Variational and related methods for the overall properties of composites. Adv. Appl. Mech. 21, 1–78.
Yeong-Moo, Y., Sang-Hoon, P., Sung-Kie, Y., 1998. Asymptotic homogenization of viscoelastic composites with periodic microstructures. Int. J. Solids Struct. 35, 2039–2055.